Akademie věd České republiky
Ústav teorie informace a automatizace, v.v.i.

Academy of Sciences of the Czech Republic
Institute of Information Theory and Automation

RESEARCH REPORT

Tomáš Mazanec

MIMO Techniques for xDSL

No. 2305 September 2011

ÚTIA AV ČR, P.O.Box 18, 182 08 Prague, Czech Republic
Tel: (+420)266052422, Fax: (+420)286890378, Url: http://www.utia.cas.cz,
E-mail: mazanec@utia.cas.cz

This report constitutes an unrefereed manuscript which is intended to be submitted for publication. Any opinions and conclusions expressed in this report are those of the author(s) and do not necessarily represent the views of the institute.

Contents

Abstract

This research report presents particular achievements and conclusions accomplished within my doctoral thesis "MIMO Techniques for xDSL". The thesis resulted from long-term research of the *Digital Subscriber Lines (DSL)* technologies and it was finished in the August of 2011.

The main thesis objective was to improve state-of-the-art techniques in the DSL systems and to develop a novel method operating on telecommunication network physical layer of DSL systems. The new method is based on the application of the *multiple-input multiple-output (MIMO)* principles commonly used in today's wireless communication systems. It resulted in direct application of the new technique exploiting MIMO features that is applicable in future implementations of the DSL physical layer.

Introduction of both initial aims and considerations that conducted the research is presented at the first chapter of this report. The key proposal of MIMO STBC scheme for DSL is presented in the second chapter. Further, two optimization strategies for scheme application in DSL transmission are presented in the same chapter. Experimental results are presented in the third chapter. Summary of my conclusions is presented in the fourth chapter.

My long-term DSL research is accompanied with several publications and software outputs that are listed in Chapter 4 "Conclusions". Later objectives of my research were presented within the thesis. Early research objectives concerned ADSL equalization techniques. In particular, two conference papers were presented in this early period: "Advanced Algorithms for Equalization on ADSL Channel" and "Simulator of ADSL Physical Layer"; and two ÚTIAs research reports were published: No. 2184 – "ADSL ekvalizační techniky", and report No. 2194 – "Simulace ekvalizérů TEQ pro ADSL toolbox".

Chapter 1

Introduction

1.1 Motivation

Digital subscriber line (DSL) technologies provide considerable share of customer's broadband access to the internet. Despite of growing customer's demands and network deployment costs, another motivation for development of wire-line broadband technologies is followed recently. Large-scale deployment of optical fiber connections, *fiber to the home (FTTH)*, within *passive optical networks (PON)* is expected to take its time [11, 36]. During a transient to full-scale FTTH and PON, wire-line broadband access technologies will have to offer competitive performance.

1.2 State of the art

Promising improvements of DSL technologies based on *multiple-input multiple-output (MIMO)* principles were developed in the last decade. According to wireless MIMO, standard scheme of single DSL links that share transmission media (cable of bonded twisted pairs) was reviewed to multiple links scheme. Further, the cross-talks, mutual disturbances between single-link transmissions, were figured as exploitable multi-path transmission known from wireless technologies. This concluded into three significant contributions to DSL: *vectored DMT (VDMT)*, *gigabit-DSL (GDSL)* and *common mode signaling (CMS)*. Targeted DSL variant is the second version of *very high speed digital subscriber lines* – VDSL2 [30], which is capable to deliver 100 Mbits/s within 30 MHz bandwidth of 250 m long twisted pair line deployed within backbone wiring of DSL network.

The first DSL improving technology, the VDMT [20, 22], applies MIMO view from network's central office (CO) and thus from one end-point only. Hence, opposite to GDSL, the VDMT can be deployed within unbonded DSL networks, where the other end-point transceivers are spatially spread (e.g.: households) and MIMO view is not applicable. VDMT enabled CO separately coordinates both upstream reception and downstream transmission by joint processing of all affiliated signals. VDMT enabled network is capable to deliver VDSL2's nominal 100 Mbit/s data-rate, however the nominal data-rate is delivered fully to each user and furthermore within less occupied bandwidth (17 MHz). The VDMT successfully progressed to international telecommunication standards for VDSL2 transceivers [31].

The GDSL [2, 3] applies MIMO view at both network end-points. Coordinated MIMO transmission is maintained at both downstream transmitter and downstream receiver, and for upstream transmission vice versa. Since transceivers have to be collocated, bonded DSL networks are the targets for GDSL deployment. Joint signal processing basically diagonalize transmission channel and thus GDSL is capable to exploit full MIMO channel capacity. GDSL link is established with a few adjacent twisted pair lines used as MIMO channel. Four twisted pair GDSL link is capable to deliver a data-rate slightly less than 1 Gbit/s. Exploiting independent transmission channels of the same GDSL link but electrically driven in common-mode, increases GDSL link data-rate to ≈1.2 Gb/s (within ≈35 MHz bandwidth of 300 m long lines).

The last DSL improving technology, the CMS, abandons traditional concept of differential mode excitation – twisted pair symmetrically driven by balanced electronic circuit, and then applies MIMO view of multiple common-mode excited links. Within the common-mode each single wire from twisted pairs cable is counted as available transmission channel and thus their number is doubled. Following MIMO view of bonded DSL network, the authors of [3] shown significant GDSL's data-rate increase when CMS is applied. Further, the CMS extension to VDMT within unbonded DSL network [34] doubled the data-rate for a single active user when it is compared to VDMT with differential mode.

1.3 Analysis

MIMO DSL systems can achieve maximal data rates that are close to the channel theory limits. These limits can be achieved within simplified system scenarios. Bonded DSL systems have much better perspective to achieve maximal rates than unbonded, where growing complexity of system scenario leads to extremely difficult task of maximizing data rate over a large number of active users. Despite of that, maximal data rate recipe is known for both bonded Gigabit-DSL and unbonded Vectored-DMT systems. Similarly to any multi-user DSL system, the data rate maximizing solution is based on proper power allocation and dynamic management of users' spectra (DSM [7, 40]). Further research on MIMO DSL systems that aims performance of different system scenarios is still ongoing ([35, 43]).

Considering DSL system from MIMO wireless point of view: each channel has the line of sight (LOS) from transmitter to receiver, far-end cross-talks (FEXT) are present and can be treated as multi-path channel propagation and channel state information (CSI) is known. DSL channels are slowly fading and slowly time-varying. Thus, advanced MIMO techniques targeting non-stationary transceivers or fast varying channel are not suitable. The principle of precoding MIMO techniques is already provided within Gigabit-DSL or Vectored-DMT concept. Beamforming techniques gain benefits from non-LOS environment and thus they would missed performance benefit of LOS environment. Spatial multiplexing methods targeted to data rate (V-BLAST) would only imitated simultaneous multi-user DSL transmission and methods targeted to error performance (D-BLAST) would lower data rate only to a fractions of achievable capacity. Summarizing wireless MIMO concepts, their usability within DSL systems and weaknesses of DSL transmission, there is a motivation opened for further research.

1.3.1 Conclusion

Research on state-of-the-art MIMO DSL technologies and wireless MIMO techniques resulted into innovative DSL scheme presented in this report. Proposed DSL scheme utilizes wireless MIMO techniques for information diversity enhancement in effort to improve transmission error rate of the state-of-the-art DSL system. Error rate improvement is maintained by transmission of redundant information instances within a *space-time block code (STBC)*. However, this method is not focused only on enhancing of regular DSL transmission, but it is capable to revive unusable channel subcarriers and thus to increase the data rate.

1.4 Aims of the thesis

To summarize the objectives of the dissertation, the list of particular aims to be achieved is provided as follows:

1. To develop a new method exploiting the MIMO *space-time block code (STBC)* technique applied to the corresponding part of the physical layer of the DSL systems.

2. To show that the proposed method improves either transmission performance or provides multiple-user access to the transmission media.

3. To present the proof of concept and to verify the proposed method by results evaluation in a standardized simulation environment.

Chapter 2

The proposed method

With the designated aims of the thesis and introductory analysis presented in the previous Chapter 1, resulting motivation is described in the first Section of this Chapter. The second Section 2.2 progressively describes the proposed scheme and concerned methods. With detailed description of wireless STBC techniques, amended with wireless application example, at the start, the proposal of the STBC application to DSL system follows in this section. This proposal is also accompanied with DSL application example for better insight. Further, the subcarriers selection algorithm is proposed for completeness of the proposed scheme. This section is concluded with simple proof of presented concept. Further considerations leading to additional development are outlined in the next Section 2.3. Starting with the second motivation to the next proposal, the DSL channel bit-loading basics and particular ”waterfilling” algorithms are described consequently. Further, the discrete loading algorithm for DSL channels is additionally described. The second method for the proposed scheme of STBC application is consequently described with the second algorithm for subcarriers selection. Finally, the proof of the second method's concept is presented in this section.

2.1 Motivation

Considering the DSL system with theoretical or practical transmission conditions, we aim to improve information transmission error rate by diversity enhancement methods known from wireless MIMO systems. The theoretical DSL system has transmission error probability given by SNR and QAM complexity on each DMT subcarrier. The practical DSL system is impaired in addition with other signals ingress and cross-talks and thus the error rates of some DMT subcarriers exceed theoretical error probability. In other words, the method's goal is to improve diversity of information transferred on error-impaired DMT subcarriers resulting in the decrease of final error rate of those subcarriers.

Based on MIMO wireless methods introduced in the previous text, space time codes (STC) are suitable for information diversity enhancement. Since trellis based STTCs are complex to decode and the DSL subcarrier would require a number of trellis code states as well as the subcarrier modulation states (up to 2^{15}), space time block codes (STBC) are the applicable choice. Precise form of information diversity addition or improvement depends on the selection of diversity coding applied. The following sections will present details of the proposed method.

2.2 Description of proposed method

2.2.1 STBC description

The STBCs encoding process starts with demultiplexing of input stream containing complex symbols (QAM symbols) to parallel substreams according to P representing the number of transmit antennas. Each parallel set consisting of P symbols is STBC encoded and resulting block of $P \times Q$ symbols is transmitted within Q symbol periods. This step is repeated continuously. Diversity added with STBCs is provided by mutual orthogonality of Q symbol sets within the transmitted block. Assuming P is the number of receiver antennas, decoding of received STBC blocks can be maintained with maximum-likelihood decoder at each block separately [18, 19]. When P complex symbols are transmitted over Q symbol periods, the STBC efficiency can be described by the *code rate* equal to fraction P/Q. The best achievable code rate for STBCs is equal to one. This code rate maximum practically means that 50 % of transmitted information is redundant or else 50 % of available space-time slots is utilized.

The STBCs are defined by an encoding matrix, which represents time domain operations (row-wise) and antenna selection (column-wise). For example Alamouti's two antenna STBC [1] is described by:

$$\mathbf{C}_2 = \begin{bmatrix} \mathbb{X}_1 & \mathbb{X}_2 \\ -\mathbb{X}_2^* & \mathbb{X}_1^* \end{bmatrix} \tag{2.1}$$

where the matrix elements $\mathbb{X}_p$ denote transmitted complex symbols, each column belongs to a specific antenna and rows represent consecutive symbols transmitted in time within one STBC block.

Beside the Alamouti's coding scheme [1] and its further enhancements proposed by Tarokh's in [41, 42], other STBC proposals are worth noting. The authors of [17] pointed to uneven power levels rising over symbols of Tarokh's multi-antenna STBCs. They proposed STBC multi-antenna scheme with equal power levels over transmitted symbols. Original Alamouti's STBC is the only one fully orthogonal code that has the code-rate equal to one and thus the best efficiency available. Other orthogonal STBCs are then less efficient. This led to the development of *quasi orthogonal space-time block codes (QOSTBC)*, which trade a part of orthogonality to gain on other properties, the code rate for example. Note that the loss of STBC's orthogonality also decreases its diversity gain. Following this approach, the authors of [33] proposed a multi-antenna QOSTBC schemes with code rate equal to one.

Table 2.1 reviews the properties of selected STBCs, namely: Alamouti's two antenna code $\mathbf{C}_2$, Tarokh's three and four antenna codes $\mathbf{C}_3$ and $\mathbf{C}_4$, the equal power variant for four antenna system $\mathbf{C}_{4\mathrm{EP}}$ and the mentioned quasi-orthogonal code $\mathbf{C}_{\mathrm{Q}4}$. The code matrices of these particular STBCs are specified in the Appendix B.

Transmission process with Alamouti's STBC (2.1) providing wireless MIMO system is depicted in Fig. 2.1. Assuming the input stream is an OFDM symbol consisting M-number of QAM symbols, the first input set has two elements, X_1 and X_2. According to STBC matrix (2.1), both antennas transmit the input symbol set unchanged (Antenna 1: X_1, Antenna 2: X_2) within the first transmitted symbol (Symbol 1). Consecutively the second symbol (Symbol 2) is transmitted, but the orthogonal set (Antenna 1: $-X_2^*$, Antenna 2: X_1^*) is submitted according to the second row of STBC matrix. Such MIMO transmission of 2×2 STBC blocks then continues with consecutive input symbols sets: (X_3, X_4), (X_5, X_6), etc. for all consecutive OFDM symbols.

Table 2.1: STBC comparison

STBC	Code-rate	No. of antennas	No. of input symbols	Code span
$\mathbf{C}_2$	1	2	2	2
$\mathbf{C}_3$	3/4	3	3	4
$\mathbf{C}_4$	3/4	4	3	4
$\mathbf{C}_{4\text{Q}}$	1	4	4	4
$\mathbf{C}_{4\text{EP}}$	3/4	4	3	4

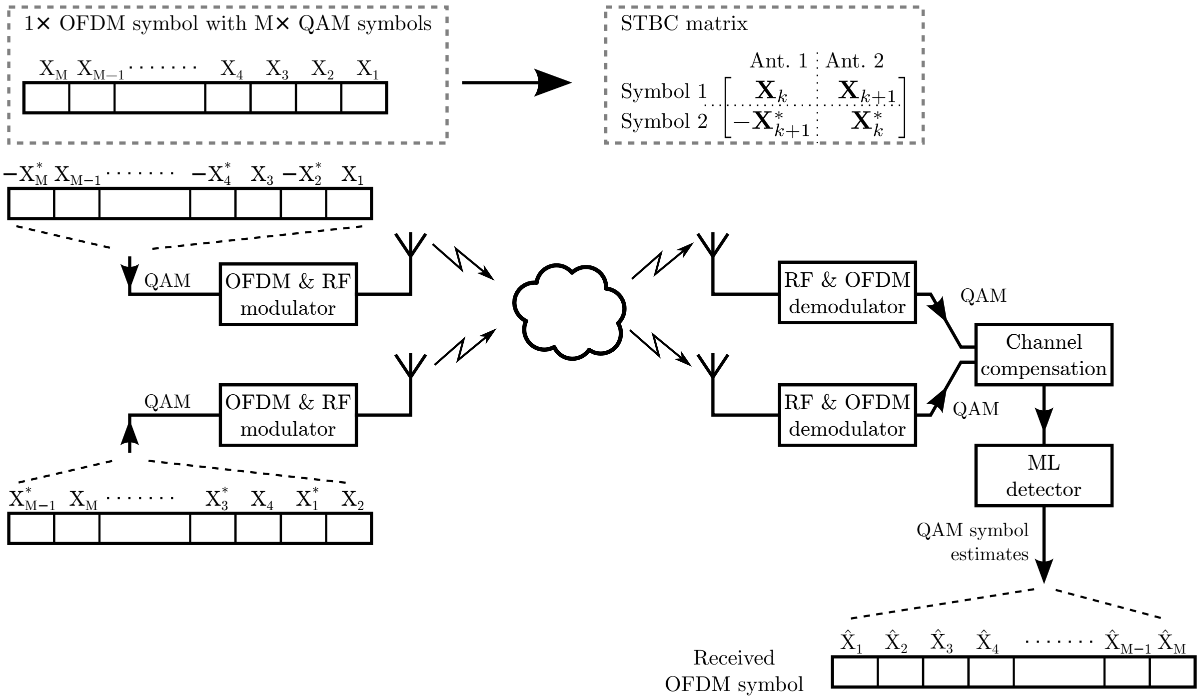

Figure 2.1: Wireless STBC application – Alamouti example

After signal demodulation, channel compensation is done and the resulting 2×2 STBC blocks of QAM symbols are processed by the maximum-likelihood detector. The transmitted symbols estimates $\hat{X}_k$ are determined with advantage of QAM symbols redundancy provided within each STBC block. This advantage results in expected improvement of transmission error performance.

2.2.2 Application to DSL system

Following the motivation presented in Section 1.3, the space-time block coding is applied to DSL system. As the DSL systems use multi-carrier modulation (DMT), the STBC application targets the DMT subcarriers. If the information diversity on selected subcarriers is increased, the error rate decrease. For the first view, subcarriers revealing error rate worse than expected are the ones selected for the STBC application.

If the DMT symbol's subcarriers resolved in frequency domain are regarded as MIMO system antennas resolved in spatial domain, the MIMO view can be applied and STBC can provide desired diversity gain. Such MIMO view of DMT symbols preserves time domain sequence, but transforms spatial diversity to frequency. In other words, proposed STBC application to DSL systems exploits frequency-time diversity instead of space-time diversity known from wireless MIMO systems. According to STBC encoding principle described above, a group of P subcarriers transfers STBC encoded block over a group of Q consecutive DMT symbols in time. Other wireless MIMO rules are also transferred to this multiple subcarriers MIMO except the utilization of other (non-selected) subcarriers. If the number of selected subcarriers is greater than number of antennas available for a given STBC, another group of P selected subcarriers serves as the next group of MIMO antennas. This multiple use of separate MIMO groups is available until the total number of subcarriers elapses. With the limited number of MIMO groups, the other subcarriers keep a regular DMT symbol transmission.

The proposed method of MIMO STBC application to DSL subcarriers essentially intercepts DMT symbol transmission within regular DSL operation and creates a bypass within the DMT transmitter and receiver. Within this bypass STBC coding and decoding operations are managed at the transmitter and receiver, respectively. Assuming all STBC groups start at the same DMT symbol, every Q-th DMT symbol takes new input QAM symbols to transmit and all other $Q-1$ of DMT symbols transmit the redundant QAM symbols' instances according to STBC prescription. This requires another, but manageable, interception to DSL data flow. Precise operation steps of this STBC application are described within the following example of Alamouti's two antenna STBC and within the formulation of subcarriers selection algorithm in the following paragraphs.

The presented MIMO STBC application targets a single DSL transmission and thus single link between DSL transmitter and receiver. The method proposed in this thesis is based on presented application and thus the method actually is: *MIMO STBC application on single DSL link.*

Application of STBC to DSL – Alamouti example

According to proposed concept of STBC application, the Alamouti's encoding matrix (2.1) will be applied on a couple of selected subcarriers and within each two consecutive DMT symbols. Precise application of the encoding matrix can be described as:

$$\begin{array}{r c} & \begin{array}{cc} \text{Subcarrier} & \text{Subcarrier} \\ k_1 & k_2 \end{array} \\ \begin{array}{r} \text{Symbol } l \\ \\ \text{Symbol } l{+}1 \end{array} & \left[\begin{array}{c:c} \mathbf{X}_{k1} & \mathbf{X}_{k2} \\ \hdashline -\mathbf{X}^*_{k2} & \mathbf{X}^*_{k1} \end{array}\right] \end{array}$$

where l is the number of DMT symbol, indices k_1, k_2 determine selected subcarriers within single MIMO group and $\mathbf{X}_k$ represents QAM symbols.

The transmission process with Alamouti's STBC providing proposed MIMO STBC application to DMT subcarriers of a DSL system is depicted in Fig. 2.2. As this example provides a two antenna system, two subcarriers have to be selected for one MIMO group. Symbol span of such STBC is equal to two and thus it is necessary to input two DMT consecutive symbols l_1, l_2. The presented example shows two MIMO groups of STBC subcarriers with indices: $k = 3, 5$ and $k = M - 2, M$, respectively. Transmission operations are mutual for all MIMO groups and thus the following process concerns only the first MIMO group with indices $k = 3, 5$.

The QAM symbols carrying data at STBC subcarriers within the first DMT symbol l_1 are extracted as input QAM symbol set ($X_3 = T_3$, $X_5 = T_5$) and encoded according to STBC's coding matrix (2.1). Resulting QAM symbol sets are inserted at the same subcarrier indices $k = 3, 5$ to all concerned DMT symbols l_1, l_2 right before DMT modulation. Note that the first DMT symbol transfers the set identical to input set and the second DMT symbol transfers the orthogonal set in the same manner as in the wireless MIMO example presented earlier. The orthogonal set in the DMT symbol l_2 is equal to $(-T_5^*, T_3^*)$.

If other MIMO groups are processed analogously, the whole transmission process is repeated for all next DMT symbol couples (l_3, l_4), (l_3, l_4), etc. The same approach of 2×2 sized STBC blocks transmission is continuously maintained on the subcarriers belonging to each MIMO group, while the input QAM symbol sets are extracted from each odd numbered DMT symbol. Note that each even DMT symbol at the transmitter's input has empty subcarriers and thus the symbol is prepared for insertion of the orthogonal QAM symbol sets. This preparation have to maintained in the DMT transmitter.

After signal demodulation (DMT), channel compensation by 1-tap frequency equalizer (FEQ) is done and the resulting 2×2 STBC blocks of QAM symbols X_k are processed by the maximum-likelihood detector. The QAM symbol estimates $\hat{X}_k$, transmitted with STBC blocks, are determined with the advantage of QAM symbols redundancy and thus with expected improvement of transmission error performance.

The regular transmission of QAM symbols T_k at subcarriers k, which are different from the ones assigned to MIMO groups, is continuously maintained. This results in complete reception of DMT symbols. The empty subcarriers depicted in the second DMT symbol l_2 at the receiver side (Fig. 2.2) denote that after the decoding of STBC blocks, the redundant information (orthogonal QAM symbol sets) were discarded for the purpose.

Comments to the method

Except the presented STBC application operations, the regular DSL transmission is assumed to be continuing.Note that some additional logic is necessary to maintain accurate operation of the presented STBC application within the physical layer of the real-world DSL system.

Proposed STBC application reveals the trade-off between transmission performance and error performance that is analogical to the wireless MIMO STBC application.

The presented MIMO view of DMT subcarriers does not include multi-user view of multiple users sharing the same transmission environment – the binder cable. The presented concept of STBC application allows to be simultaneously operating within different users, but other users' cross-talks are not manageable and thus they cause alien impairments.

The selection of STBC targeted subcarriers should be provided with some reasoning given by an algorithm. Analysis of per-subcarrier error rate of received DMT symbols seems to be suitable approach. The algorithm for subcarriers selection can vary in the choice which directly-neighbouring or which further-placed subcarriers are suitable for a MIMO group.

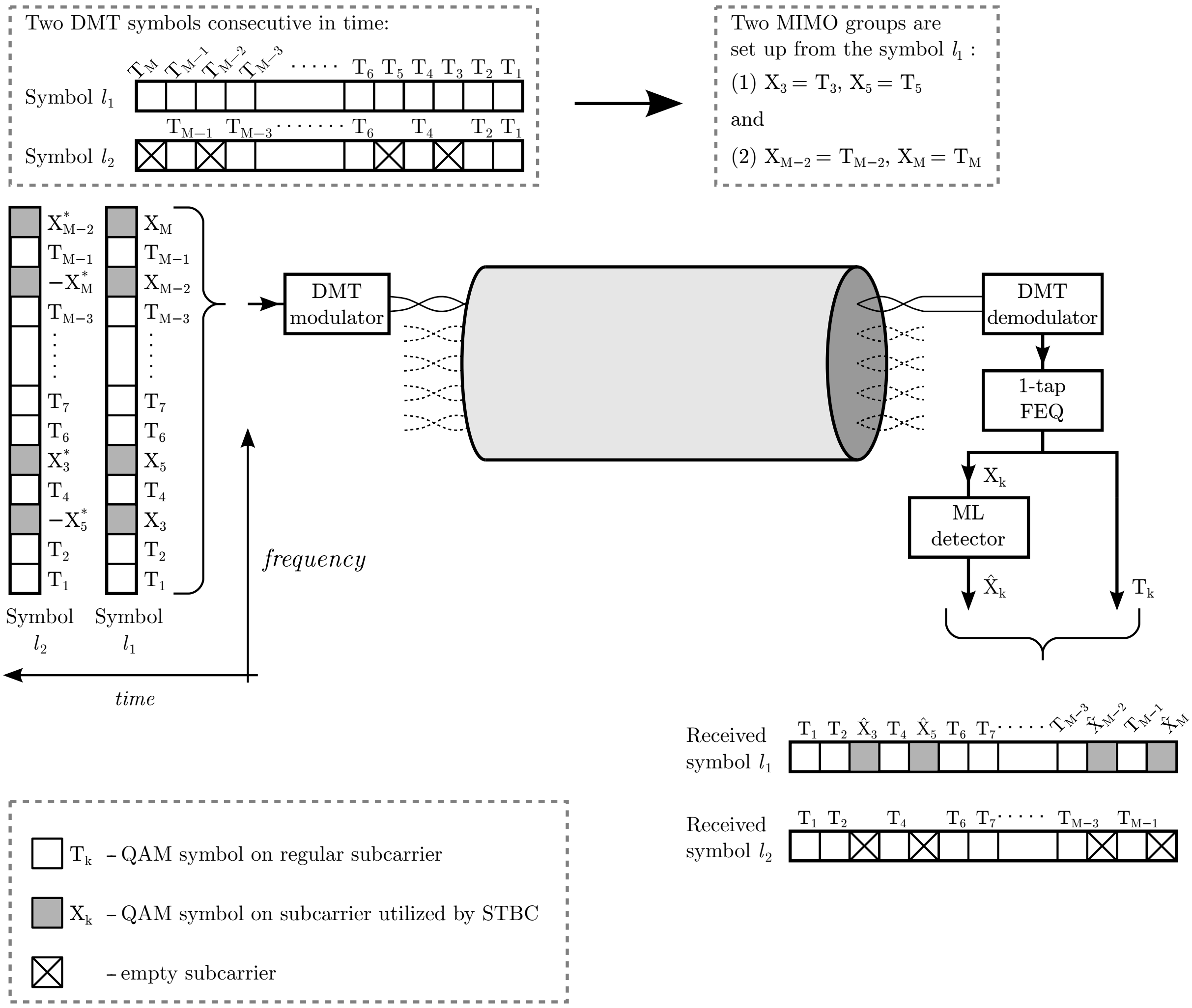

Figure 2.2: Single link DSL application of STBC – two MIMO groups with Alamouti's STBC example

2.2.3 Subcarriers selection algorithm based on error feedback

The following approach provides a reasonable link between DSL transmission error rate and configuration of subcarriers within the proposed STBC application. The aim of this algorithm is to improve error performance of DSL transmission according to the motivation presented in Section 1.3.

The goal is accomplished by subcarrier error analysis of the first L DMT symbols transmission and further set up of MIMO groups, which finally include all erroneous subcarriers that results in error count greater than the threshold. After each L DMT symbols transmission with MIMO STBC enabled, new subcarrier error analysis is done and the resulting set of erroneous subcarriers is logically added to the previous set. Then the DMT symbols transmission is repeated with the updated MIMO groups and this process continues repetitively.

If the targeted DSL system's error rate is caused by some effects that are manageable by the proposed STBC application, the resulting error rate will be decreased to the level of threshold.

Assuming the specific STBC with P antennas and Q symbols span is selected, desired error count Pe is determined and initial conditions are set:

Error feedback subcarriers selection algorithm

---

1. Analyse error count of L received DMT symbols per each subcarrier.
2. For a given error count threshold Pe, find all indices k of subcarriers, which showed error count greater than the threshold:
```
SetK_old = SetK;
SetK = find(ERRk >= Pe);
SetK = SetK OR SetK_old;
Knum = lenght(SetK);
```
3. Enumerate how many MIMO groups are necessary to include $Knum$ subcarriers for a given number of STBC antennas P:
```
Mcount = floor (Knum / P);
reminder = Knum - Mcount * P;
if (reminder/P) > 0.5
then
         Mcount = Mcount + 1;
endif
```
4. Attach each P subcarrier indices found in the Step 2. to a MIMO group in ascending order:
```
for i=1:Mcount
         MIMOset[i] = SetK[(i-1)*P+1:i*P];
endfor
```
5. Configure and run DSL transmission with MIMO groups encoding the data by STBC.
6. After L DMT symbols transmitted proceed to the Step 1.

2.2.4 Proof of concept

Foundations of STBC concept validity origin from Alamouti's work [1] and related research in diversity coding area. For the case of the proposed method it can be briefly proven that the concept of diversity coding with STBC is valid also for the DMT based DSL systems.

Error probability function for a multi-carrier digital communication systems using square constellations of quadrature modulation on DMT subcarriers was derived in several DSL textbooks. Let us consider the error probability function [9, 40] for such a communication system given by:

$$(P_e)_k \approxeq \mathcal{Q}\left[\sqrt{\frac{3 \cdot \mathrm{SNR}_k}{M-1}}\right] \tag{2.2}$$

where SNR_k denotes the signal to noise ratio, M is the number of QAM states for each subcarrier k and $\mathcal{Q}[\cdot]$ denotes the Q function (Please refer to the Appendix A.5).

Assuming P is the number of subcarriers subjected to transfer Q independent instances of information according to STBC principle, two extreme scenarios of overall error probability can arise:

1. Worst case: all information instances are received erroneous.
2. Best case: all information instances are received without an error.

For a successful information transmission the worst case is relevant so that the error probability of the worst case is given by:

$$P_{eW} = \frac{1}{Q} \cdot \frac{1}{P} \sum_{k=1}^{P} (P_e)_k \tag{2.3}$$

Assuming that the correct configuration of DMT subcarriers is provided by the bitloading within DSL system, the target error probability of each subcarrier will be approximately equal $P_{eT} = (P_e)_k,\ k = 1 \dots P$, and thus the worst case error probability (2.3) become:

$$P_{eW} = \frac{1}{Q} P_{eT} \tag{2.4}$$

A successful information transmission is not accomplished with probability given by (2.4) and thus the proof concludes in observation that:
Using the STBC diversity to transfer Q independent information instances leads to the error probability Q-times lower than the error probability of a single subcarrier transfer.

2.3 Further development and description of the second proposed method

Research accompanying this thesis includes also an extensive knowledge of DSL systems especially Asymmetric-DSL systems. Revealing the advantages of diversity based MIMO techniques like space-time coding, another DSL system enhancement is possible. This enhancement also utilize space-time coding principles giving the diversity gain, but it targets different scenarios of DSL system transmission.

If a DSL system determines capabilities of its transmission channel, a number of transferable bits is enumerated for each subcarrier according to regular bitloading procedure [9, 40]. The bitloading process can reveal that some DMT subcarriers are not able to transfer information due to poor SNR conditions. The constraint of target error probability figures in the bitloading computations and thus the unavailability of certain subcarriers depends on the error performance constraint. As the diversity gain of STBC encoding allows to improve error performance, these unavailable subcarriers can be re-enabled under specific conditions described later.

2.3.1 Motivation of the second method

With the ability to increase diversity of transmitted information and thus the error performance on DSL system's DMT subcarriers, we can improve information transmission on those DMT subcarriers that are considered to be insufficient for information transmission. The bitloading process results in transferable bits of information for each DMT subcarrier and the least applicable amount is indeed one bit. If unavailable DMT subcarriers are determined to carry less than one bit but more than zero bits, they can be presented as subcarriers that can transfer one bit of information, but with lower error performance than constrained within bitloading. These observations conclude in statement that: If P number of DMT subcarriers can carry each one bit of information with a low error performance, the same DMT subcarriers can carry one bit again but with higher error performance maintained by Q independent instances of information according to STBC principle. This approach also shows the error versus transmission performance trade-off revealed within the previously proposed method in Section 2.2.

The scheme of the MIMO STBC application on a single DSL link, presented earlier in Section 2.2, fits for purposes of this second approach. The subcarriers selection will have to be provided by a different procedure.

2.3.2 Channel bitloading

Within initialization of a DSL system transmission, the bit-loading is done. The bitloading is the state of the art approach giving an optimal transmission set up for the analyzed transmission channel. For a determined channel's per-subcarrier SNR, a number of bits and gain level are enumerated for each subcarrier. This approach is based on parallel multiple discrete channels theory, which describes multi-carrier modulated signals, and reveals the Shannon's capacity of the channels, i.e.: subcarriers [9, 40].

Assuming the channel model in frequency domain [9, 40], a single AWGN channel with gain H_k and noise power spectral density σ_k^2 has a maximum data rate capacity given by:

$$\bar{b}_k = \frac{1}{2}\log_2\left(1 + \frac{\text{SNR}_k}{\Gamma}\right) \text{ [bits/dimension] , with: } \text{SNR}_k = \frac{\varepsilon_k \cdot |H_k|^2}{\sigma_k^2} \text{ [-]} \tag{2.5}$$

for each subcarrier $k = 1 \ldots N$. Furthermore, an additional subcarrier gain is provided within ε_k and Γ denotes the SNR gap that ensures targeted error probability of QAM (PAM) modulated subcarrier. The SNR gap for a discrete multi-channel transmission at given error probability P_e can be approximately given by:

$$\Gamma \approxeq \frac{1}{3}\left(\mathcal{Q}^{-1}[P_e]\right)^2 \text{ , [-]} \tag{2.6}$$

where $\mathcal{Q}^{-1}[\cdot]$ denotes inverse of the Q function[1]. For example of an uncoded QAM and the error probability $P_e = 10^{-6}$ the SNR gap Γ is constant at 8.8 dB. Note that in the DSL systems, the SNR gap might be decreased by a coding gain γ_c provided by a coding technique and might be increased by an inserted safety reserve, the SNR margin γ_m, and thus overall SNR gap would be $\Gamma_{TOT} = \Gamma \cdot \gamma_m / \gamma_c$ [-].

With the DMT modulation, the N real subchannels can be revealed as $K = N/2$ complex subchannels and thus the maximum data rate (2.5) for a DMT complex subchannel can be written as:

$$b_k = \log_2\left(1 + \frac{\text{SNR}_k}{\Gamma_{TOT}}\right) \text{ [bits]} \tag{2.7}$$

Maximum data rate of a DMT symbol is then equal to sum of all subchannels data rates:

$$R = \sum_{k=1}^{N} \bar{b}_k = \sum_{k=1}^{K} b_k \tag{2.8}$$

Waterfilling

The optimal bitloading is generally achieved with so-called "Water-filling" principle. For the DMT systems, the optimal bitloading is achieved when transmitted subcarrier energies ε_k satisfy ([9]):

$$\varepsilon_k + \Gamma \cdot \frac{\sigma_k^2}{|H_k|^2} = \text{constant} \tag{2.9}$$

for each subcarrier k.

Such a condition (2.9) leads to a set of linear equations with boundary constraints. There are two types of loading algorithms - those that try to maximize data rate and those that try to maximize performance at a given fixed data rate. Other water-filling algorithms are mostly derived from these two types. The publications of J. Cioffi [9] are recommended for further reading.

Rate-Adaptive loading criterion, maximizes (or approximately maximizes) the number of bits per symbol subject to a fixed energy constraint. Margin-Adaptive loading minimizes (or approximately minimizes) the energy subject to a fixed number of bits per symbol constraint. Further description of these waterfilling algorithms can be found in [9, 40].

[1] Please refer to the Appendix A.5

Discrete loading

Water-filling algorithms result in bit distributions where b_k can be any real number. Alternative loading algorithms allow the enumeration of bit distributions that are more flexible to implementation with a finite granularity [9]. The granularity of a multi-channel transmission system is the smallest incremental unit of information that can be transmitted. Further description of the discrete loading algorithm can be found in [9].

2.3.3 Description of the second method

According to the motivation presented at the start of this section, the same scheme of the MIMO STBC application on a single DSL link is used with the only difference in the method of subcarriers selection. Subcarriers disabled by bitloading due to insufficient SNR are the targets to the selection.

For the first view, it is assumed that the channel bitloading is accomplished with some waterfilling method as presented in the previous text. Result of bitloading procedure, amount of bits transferable per each subcarrier, is determined according to information capacity of each subcarrier (2.5) and with target error probability constraint (2.6). The result is usually a vector of real numbers $\bar{b}_k$, and its rounded representation is used for the set up of QAM within subcarriers. Precisely for a QAM at DMT subcarriers bitloaded with (2.7) is the set up given by:

$$\tilde{b}_k = \text{round}(b_k) = \text{round}\big(2 \cdot \bar{b}_k\big) \quad \text{[bits]}.$$

An illustrative example of the bitloading vector, defined in (2.7), for a few DMT subcarriers of a DSL channel is depicted in Fig. 2.3. Difference between the bitloading vector, $\bar{b}_k$, and rounded representation is noticeable within the most of depicted subcarriers. The disabled subcarriers, where the rounded bitloading resulted in zero bits, are the possible targets for selection, but it is necessary that each disabled subcarrier have some amount of information capacity to be utilized. Since the bitloading vector, $\bar{b}_k$, represents the information capacity, subcarriers with the bitload values greater than zero are the targets for selection. In summary, there are two depicted subcarriers (with indices $k = 16$ and 23) satisfying introduced conditions of selection.

Together with the bit assignment vector, $\bar{b}_k$, a subcarrier energy gains, ε_k, are provided by the bitloading. If a subcarrier can be reasonably amplified to achieve next integer amount of bits per dimension, its energy gain is increased and vice versa. This energy gain adjustment compensates possible rounding error.

Following the motivation presented at the start of this section, subcarriers showing SNR insufficient enough to carry one bit of information with given error probability constraint are the target of selection to the MIMO STBC application on single DSL link. Error probability analysis within the bitloading is necessary to select a P number of subcarriers to carry a Q independent instances of information according to STBC principle. Instead of error probability analysis, the bitloading vector $\bar{b}_k$ can be used to determine targeted subcarriers if a correct upper and lower bounds of $\bar{b}_k$ elements are determined under the error probability constraint. A correct bitloading of the subcarriers is required for the following derivation. Hence it is assumed that the energy gains for disabled subcarriers have default values, i.e.: $\varepsilon_k = 1$ and the error probability of each subcarrier is given by the targeted error probability:

$$(P_{eD})_k = P_{eT} \ , \ \ k = 1 \dots N \tag{2.10}$$

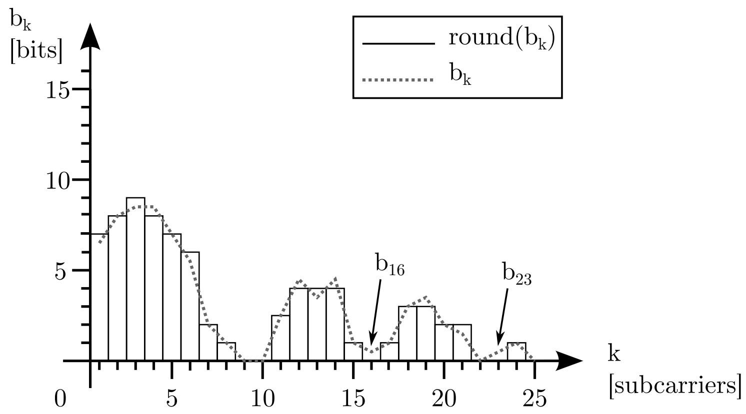

Figure 2.3: Illustrative example of channel bitloading.

where $(P_{eD})_k$ denotes a default error probability.

With observations of waterfilling based bitloading from the above paragraph, an upper bound for $\bar{b}_k$ is clearly 0.25 and thus subcarriers with $\bar{b}_k < 0.25$ are selected in the first step.

Let us determine the lower bound for selected subcarriers. Error probability of k-th subcarrier bitloaded with $\bar{b}_k$ bits per dimension, as defined in (2.5), is related to subcarrier's SNR:

$$(P_e)_k \approxeq \mathcal{Q}\left[\sqrt{\frac{3 \cdot \mathrm{SNR}_k}{M-1}}\right] \tag{2.11}$$

where M-state QAM modulation with $M = 2^{2 \cdot \bar{b}_k}$ is applied on the k-th subcarrier and $\mathcal{Q}[\cdot]$ denotes the Q function[2].

To maintain the STBC principle valid, the selected subcarriers error probability has to be at the most Q-times higher than the target error probability P_{eT} given by the constraint (2.7) and thus:

$$(P_e)_k \leq Q \cdot P_{eT} \tag{2.12}$$

When the SNR_k is expressed from the (2.11) and incorporated to (2.5) the bitloading equation becomes:

$$\bar{b}_k = \frac{1}{2}\log_2\left(1 + \frac{(M-1)\cdot 1/3 \cdot \left(\mathcal{Q}^{-1}[(P_e)_k]\right)^2}{\Gamma_T}\right) \text{ [bits/dimension]} \tag{2.13}$$

where Γ_T denotes the SNR gap (2.6) for a system constrained with P_{eT}.

Selected subcarriers will carry one bit of information, i.e.: $\bar{b}_k = 0.5$ and $M = 2$, and thus the (2.13) with the substitution of (2.12) become the expression giving the desired lower bound:

$$\bar{b}_{\mathrm{LOW}} = \frac{1}{2}\log_2\left(1 + \frac{1/3 \cdot \left(\mathcal{Q}^{-1}[Q \cdot P_{eT}]\right)^2}{\Gamma_T}\right) \text{ [bits/dimension]} \tag{2.14}$$

It the targeted system employs the SNR reserve, so-called "margin", γ_m, the resulting

[2]Please refer to Appendix A.5

lower bound (2.14) can be even decreased to:

$$\bar{b}_{\text{LOW}} = \frac{1}{2}\log_2\left(1 + \frac{1/3 \cdot \left(\mathcal{Q}^{-1}[Q \cdot P_{eT}]\right)^2}{\Gamma_T \cdot \gamma_m}\right) \text{ [bits/dimension]} \tag{2.15}$$

With the upper and lower bounds determined an algorithm for subcarriers selection can be established. The selected subcarriers have indices k that corresponds to elements of the bitloading vector satisfying:

$$\bar{b}_{\text{LOW}} \leq \bar{b}_k < 0.25 \tag{2.16}$$

Comments to the method

Considering the accuracy of the lower bound enumeration, the equation (2.11) is indeed approximate, but it is sufficiently accurate for DMT systems using even- and odd-bit square constellations of QAM symbols [9].

Analysis of the lower bound $\bar{b}_{\text{LOW}}$ values from (2.14) shown that for a small number of Q information instances, common with the wireless STBCs, the lower bound values are undesirably close to the constraint $\bar{b}_k = 0.5$ and thus they are unusable. With application of the margin, γ_m, the lower bound values (2.15) are valid. Example results of the lower bound enumeration at given error probability constraints and with additional margin application[3] are presented[4] in Table 2.2. Note that the values in the second column, $\bar{b}_{\text{LOW}}$, are not applicable since they are above the upper bound $\bar{b}_{\text{UP}} = 0.25$.

Table 2.2: Lower bound for $(P_e)_k = Q \cdot P_{eT}$ and $P_{eT} = 10^{-6}$.

Q	$\bar{b}_{\text{LOW}}$	$\bar{b}_{\text{LOW}}$ @$\gamma_m = 2.5$	$\bar{b}_{\text{LOW}}$ @$\gamma_m = 4.0$
1	0.50	0.24	0.16
2	0.48	0.23	0.15
3	0.47	0.22	0.15
4	0.46	0.22	0.14
8	0.43	0.20	0.14

Observed span between valid lower and upper bounds is quite tight. When a transmission on re-enabled subcarriers is satisfactory with a distinctively lower error performance, the subcarrier's error probability ratio (2.12) can be changed. For example of the same Q instances of information and the selected subcarriers error probability equal to: $(P_e)_k = 10^3 \cdot Q \cdot P_{eT}$ constrained with $P_{eT} = 10^{-6}$, the lower bound values were enumerated and presented[5,6] in Table 2.3.

Note that the determined lower bound (2.14), and (2.15) respectively, also represents the lowest error performance of subcarriers that can be re-enabled.

[3]Practical margin values are considered: 2.5 (4dB) for ADSL and 4.0 (6dB) for VDSL [4]
[4]Resulting $\bar{b}_{\text{LOW}}$ values are rounded to a two digits.
[5]Practical margin values are considered: 2.5 (4dB) for ADSL and 4.0 (6dB) for VDSL [4]
[6]Resulting $\bar{b}_{\text{LOW}}$ values are rounded to a two digits.

Table 2.3: Lower bound at different $(P_e)_k$ constraint:
$(P_e)_k = 10^3 \cdot Q \cdot P_{eT}$ and $P_{eT} = 10^{-6}$.

$10^3 \cdot Q$	$\bar{b}_{\text{LOW}}$	$\bar{b}_{\text{LOW}}$ @$\gamma_m = 2.5$	$\bar{b}_{\text{LOW}}$ @$\gamma_m = 4.0$
1000	0.25	0.11	$7.2 \cdot 10^{-2}$
2000	0.23	$9.8 \cdot 10^{-2}$	$6.4 \cdot 10^{-2}$
3000	0.21	$9.0 \cdot 10^{-2}$	$5.8 \cdot 10^{-2}$
4000	0.20	$8.4 \cdot 10^{-2}$	$5.4 \cdot 10^{-2}$
8000	0.16	$7.0 \cdot 10^{-2}$	$4.5 \cdot 10^{-2}$

It is assumed that the energy gains ε_k from bitloading are kept valid and applied to the transmission. The re-enabled subcarriers keep their energy gains unchanged (equal to one) with reason to not interfere the energy constraint of a waterfilling based bitloading.

Bitloading constraint of one bit ($\bar{b}_k = 0.5$) applied to re-enabled subcarriers in (2.13) is higher than the upper bound $\bar{b}_{\text{UP}} = 0.25$, but it is correct. In comparison to a waterfilling based bitloading, the proposed STBC application scheme does not boost subcarriers' energies and thus it can not increase subcarrier's capacity to one bit in the same manner as the bitloading does. Note that modifications to the energy allocation break an optimal bitloading of the DSL channel.

Above derivation of the lower bound is assumed for a waterfilling based bitloading. With discrete loading algorithms, which recognize finite information granularity, the bitloading results break the presented concept of $\bar{b}_k$ bounds with their integer distribution of bits. Nevertheless, the presented approach of disabled subcarriers reuse is valid when the SNR margin is applied to the DMT transmission. This reserve gives an equivalent SNR gain to be exploited. Selection of subcarriers is then decided according to upper bound only. The upper bound value is equal to discrete loading algorithm's granularity of information and thus it is $\bar{b}_{\text{UP}} = 0.5$ [bit/dimension] for square QAM constellations [9]. Resulting error probability of transmission on reused subcarriers has a complex relation to discrete loading algorithms and it is not provided here.

2.3.4 Subcarriers selection algorithms based on bitloading feedback

Following algorithms represent reasonable decision of subcarriers selection for the proposed STBC application. The effort of these algorithms is to enable an information transmission on DMT subcarriers that were disabled by bitloading due to insufficient SNR conditions. The aim of this approach is to improve the DSL transmission performance according to the motivation presented at the beginning of this section.

The aim is accomplished by analysis of bitloading results before a start of the DSL transmission and further set up of MIMO groups, which finally include all subcarriers suitable to reuse. This set up is valid until a new initialization of DSL transmission and thus a new bitloading occurs. When such an event happens, the bitloading results analysis and the MIMO groups set up are repeated to begin next DSL transmission.

With the observations of bitloading vector use to subcarriers selection, a two different algorithms were proposed. The first algorithm targets a system with applied SNR margin and it maintains the error probability constraint on selected subcarriers (2.12) with use of both bitloading vector bounds (2.16). The second algorithm employs only the upper bound for bitloading vector and thus it results in much lower error performance $((P_e)_k >> Q \cdot P_{eT})$ on selected subcarriers. The SNR margin can be applied in the target system.

Assuming the specific STBC is applied to P subcarriers and its code is spanning Q consequent DMT symbols, the lower and upper bounds for bitloading vector at given error probability constraint are determined and initial conditions are set, the algorithm operates as:

Bitloading feedback subcarriers selection algorithm 1

---

1. Analyse bitloading vector $\bar{b}_k$.
2. Select subcarriers whose bitloading satisfies: $\bar{b}_{\text{LOW}} \leq \bar{b}_k < \bar{b}_{\text{UP}}$, and enumerate their count $Knum$.
3. Enumerate how many MIMO groups are necessary to include $Knum$ subcarriers for a given number of STBC subcarriers P:
```
Mcount = floor (Knum / P);
reminder = Knum - Mcount * P;
if (reminder/P) > 0.5
then
        Mcount = Mcount + 1;
endif
```
4. Attach each P subcarrier indices found in the Step 2 to a MIMO group in ascending order:
```
for i=1:Mcount
        MIMOset[i] = SetK[(i-1)*P+1:i*P];
endfor
```
5. Configure and run DSL transmission with MIMO groups encoding the data by STBC.
6. When DSL transmission and the bitloading re-initialize, proceed to the Step 1.

Assuming the specific STBC is applied to P subcarriers and its code is spanning Q consequent DMT symbols, the upper bound for bitloading algorithm is determined and initial conditions are set, the algorithm operates as:

Bitloading feedback subcarriers selection algorithm 2

---

1. Analyse bitloading vector $\bar{b}_k$.
2. Select subcarriers whose bitloading satisfies: $\bar{b}_k < \bar{b}_{\text{UP}}$, and enumerate their count $Knum$.

3. – 5. Proceed the same steps as the Algorithm 1.

6. When DSL transmission and the bitloading re-initialize, proceed to the Step 1.

2.4 Conclusions

Proposed scheme of the STBC MIMO application to a single DSL link employs a MIMO view of the DMT subcarriers in frequency-time manner, which is in contrast with general space-time MIMO view known from wireless transmission environment. Adopted concept of information diversity provided by STBC that allows error performance improvement is not broken with application to DMT subcarriers with the assumptions that the subcarriers are independent and a non-alien FEXT is only present cross-talk.

Two methods providing scheme setup by selection of DMT subcarriers for the STBC encoding are proposed. The first method directly targets the increase of error performance and the subcarriers selection is driven by subcarrier's error rate. Within this method, the subcarriers are STBC encoded in the case where their error rate exceeds a given threshold. The second method applies the STBC encoding on subcarriers, which were disabled by bitloading due to insufficient information capacity. The first method is applicable in general and the second is targeted to DSL channels with poor SNR conditions at a non-negligible number of subcarriers.

Presented concept of STBC application allows to be applied simultaneously to different users, but the cross-talks from users are not managed.

Chapter 3

Experiment results

This chapter presents numerical results of described MIMO STBC application on single DSL link. The aim is to confirm improvements expected with application of the proposed scheme. Both methods for subcarriers selection provided within the scheme: Error feedback and Bitloading feedback were included in experiments and thus both high SNR and low SNR instances of the DSL transmission were evaluated. Moreover, both scheme methods were evaluated for referential channel model and for channel based on real measurements of DSL metallic cable – "real channel".

The referential setup of DSL transmission was developed aiming theoretical and non-disturbed transmission system. Otherwise the real channel setup targeted a transmission system dealing with real signal impairments. This second setup utilizes the "real channel" and has the functionality of initialization with DSL training sequence, channel estimation and noise power spectral density estimation. Further, this real channel setup provides parallel transmissions to simulate a multi-user DSL system with STBC scheme applied to each user.

The MIMO STBC scheme was evaluated[1] within standardized simulation environment (Mathworks Matlab). Additionally to proposed scheme functionality, all appropriate function blocks of the DSL physical layer were developed and proper DSL transmission was simulated. Detailed description of DSL transmission concerning physical layer can be found in [4, 40]. Extension of the MIMO STBC functionality was optionally disengaged to maintain unimpaired DSL transmission, which was initial simulation within each experiment.

[1]Experiments were evaluated numerically by the bit error ratio (BER), given by fraction of erroneous bits count and total bits count. Further evaluations use the symbol error ratio (SER), given by fraction of erroneous subcarrier symbols count and total DMT symbols count.

3.1 Referential experiments

These experiments were performed to establish results related to theoretical expectations. DSL channel was modeled by a simple linear-phase finite impulse response (FIR) filter, channel impairments were induced only by an additive white Gaussian noise (AWGN), prior channel knowledge and perfect synchronization at receiver were assumed.

3.1.1 Method with the error feedback

According to the MIMO STBC scheme application by the first method, the setup for a high SNR transmission and the Error feedback algorithm (see Section 2.2.3) were established. Following DSL transmission parameters were set within the simulation:

Signal to noise ratio	SNR=50 dB
SNR gap	$\Gamma = 8.8$ dB
Target error probability	$P_{eT} = 10^{-6}$
SNR margin	$\gamma_m = 0$
Channel bandwidth	f=1.104 MHz
Subcarriers spacing	Δf = 4312.5 kHz
No. of available subcarriers	K=255
Bitloading	RA waterfilling

Frequency response of the channel FIR filter model and consequently determined bitloading of the channel with the given configuration are depicted in Figure 3.1.

Achieved results of this experiment with 8 000 DMT symbols transferred are summarized in Table 3.1. Reference DSL transmission with disabled STBC functionality resulted in transfer of $\approx 28.7 \cdot 10^6$ bits and shown the bit error rate: BER=$3.58 \cdot 10^{-6}$. Consecutive columns in the table shows the resulting rate and BER for a different STBCs applied to the transmission. Resulting values corresponds to expected improvement that BER is decreased with cost of an amount of bit rate. For example of the C2 code, the resulting BER is decreased to 53 % at cost of bit rate fall to 94 %. Note that this C2 code application was maintained within fifteen MIMO groups at total number of thirty subcarriers (see the bottommost row of the table).

Further parameters of data transmission are presented within the table of results: Bits/symbol – precise number of bits carried in one DMT symbol, Symbol errors – number of QAM symbols impaired with some bit error and Symbol error rate (SER) related to the total number of transferred DMT symbols.

Following graphs show the experiment results presented in the Table 3.1 and corresponding selection of subcarriers based on the error feedback. The reference transmission (Fig. 3.2) shown bit errors at depicted subcarriers and thus the error feedback algorithm selected these subcarriers to STBC application. Subcarriers utilized by the given STBC and symbol errors resulting after DSL transmission are depicted in the following graphs: 3.3, 3.4, 3.5, 3.6, 3.7, for the following STBCs: C2 – Alamouti's two antennas, C3 and C4 – Tarokh's three and four antennas, C4EP – equal power modification of four antennas code and QC4 – quasi-orthogonal

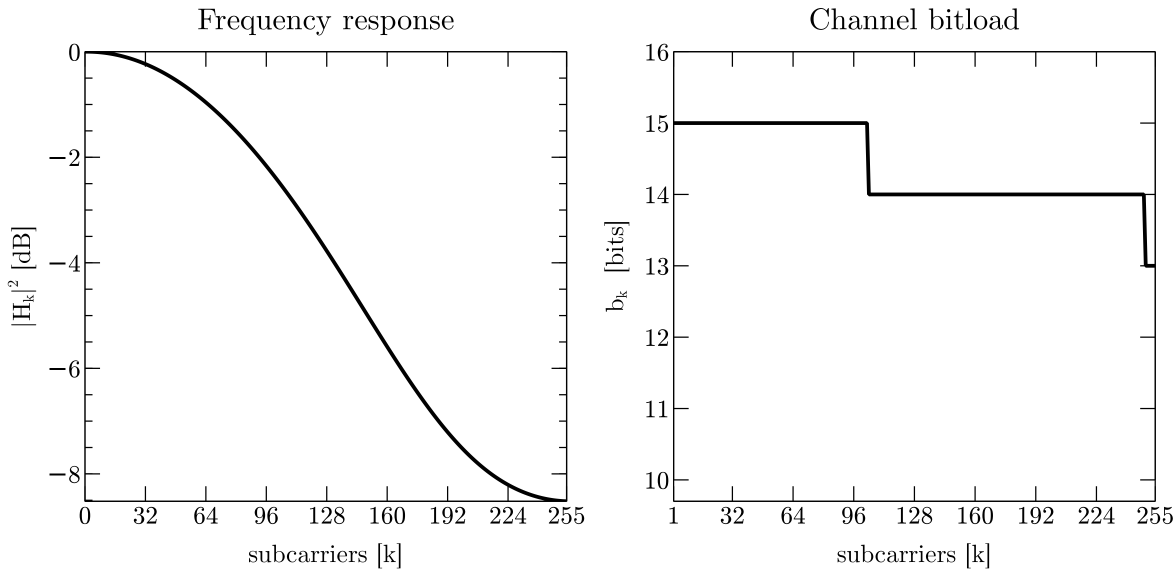

Figure 3.1: Frequency response and bitloading of the selected channel model.

Table 3.1: Error feedback results for 8 000 DMT symbols transmitted.

	Reference	C2	C3	C4	C4EP	QC4
Rate [10^6 bits]	28.7	27.1	26.2	26.2	26.2	26.4
Bits/symbol [bits]	3592	3382	3277	3274	3274	3298
BER [-]	3.58E-06	1.89E-06	1.56E-06	1.53E-06	1.95E-06	1.71E-06
Symbol Errors [symbols]	47	24	24	21	19	22
SER [-]	5.88E-03	3.00E-03	3.00E-03	2.63E-03	2.38E-03	2.75E-03
No. of STBC subcarriers	0	30	30	28	28	28

four antennas code. Note that the most of STBC experiments did not shown any errors below 160th subcarrier and thus the relevant bandwidth is depicted in each graph.

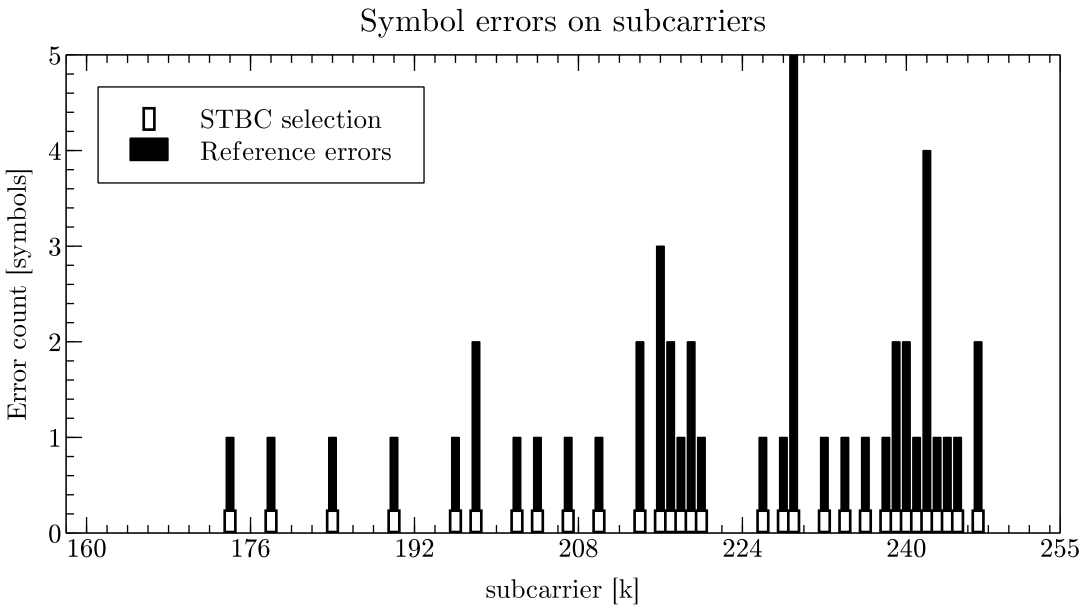

Figure 3.2: Reference transmission and subcarriers selection.

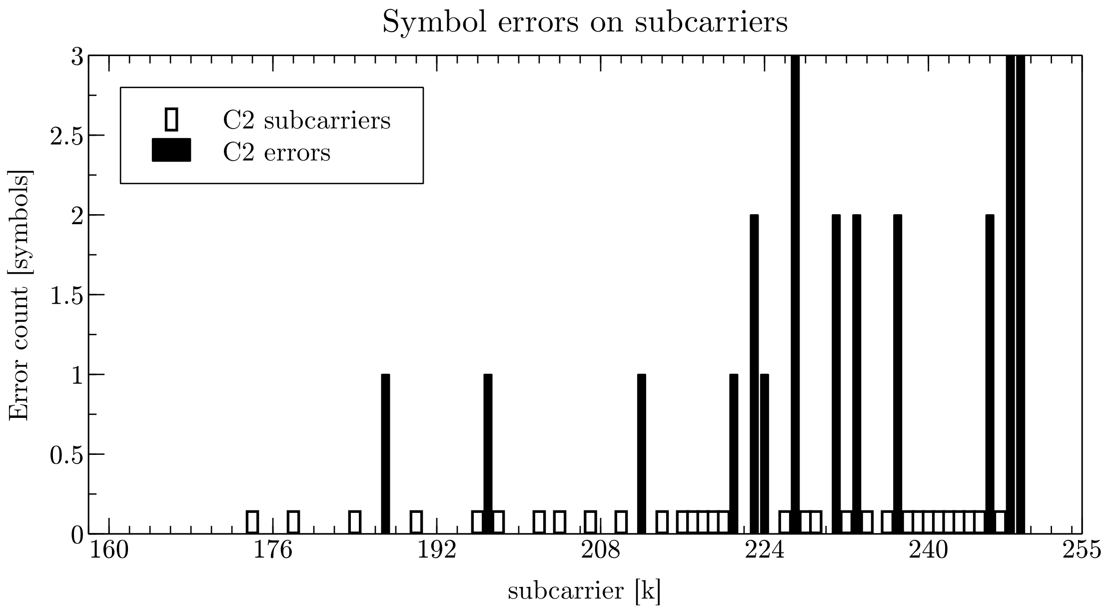

Figure 3.3: Transmission with C2 STBC and selected subcarriers.

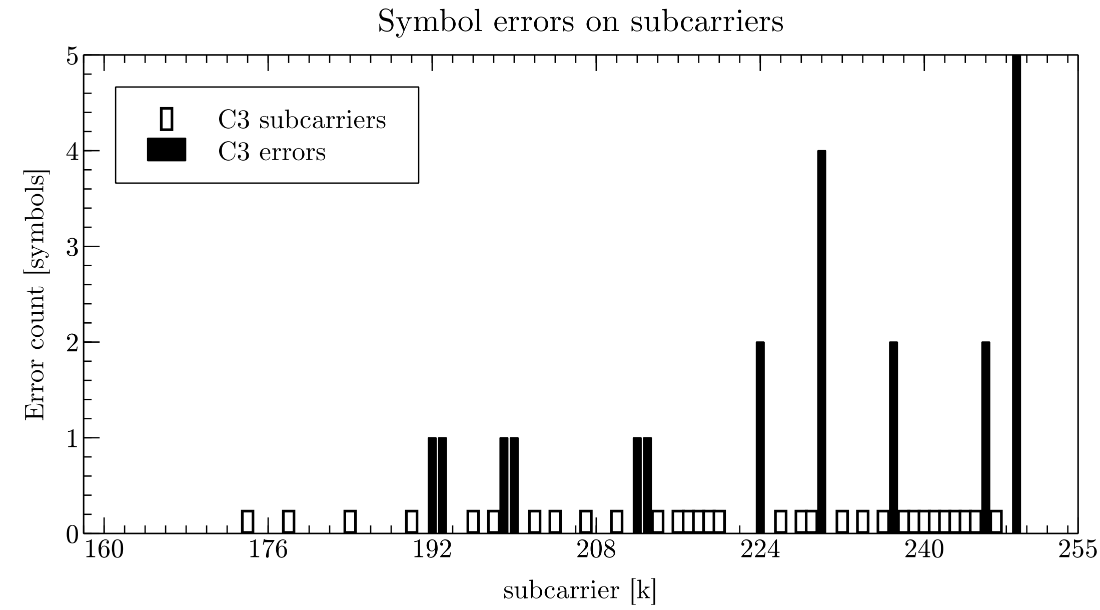

Figure 3.4: Transmission with C4 STBC and selected subcarriers.

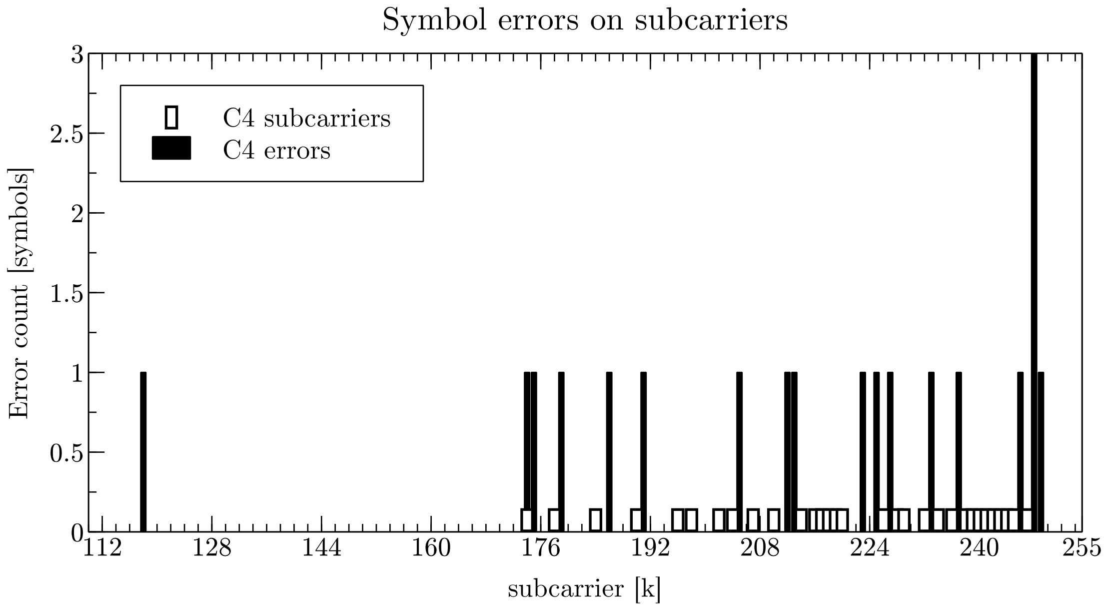

Figure 3.5: Transmission with C4 STBC and selected subcarriers.

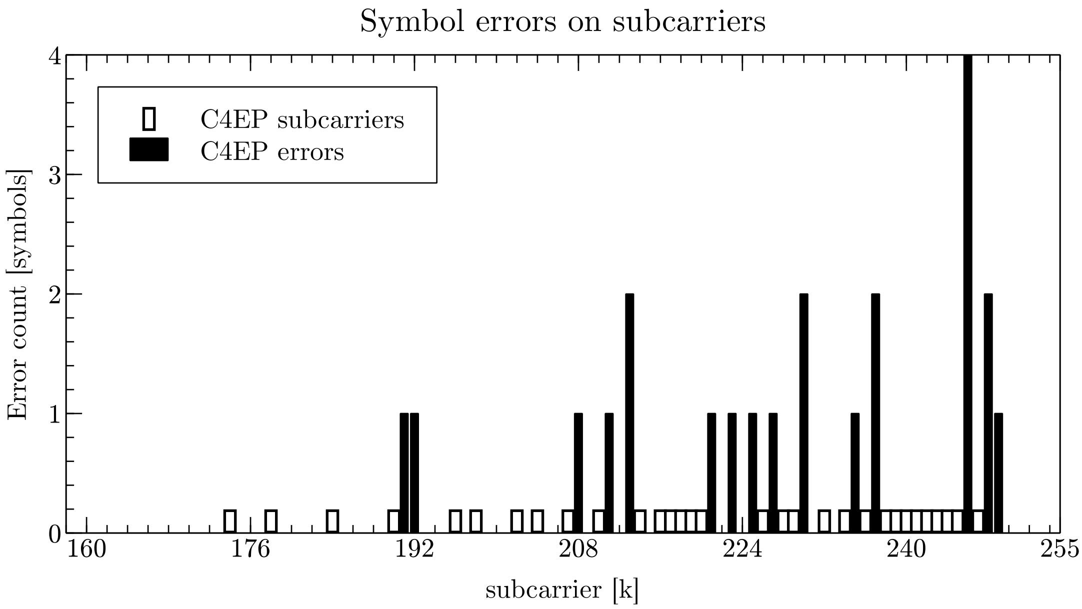

Figure 3.6: Transmission with C4EP STBC and selected subcarriers.

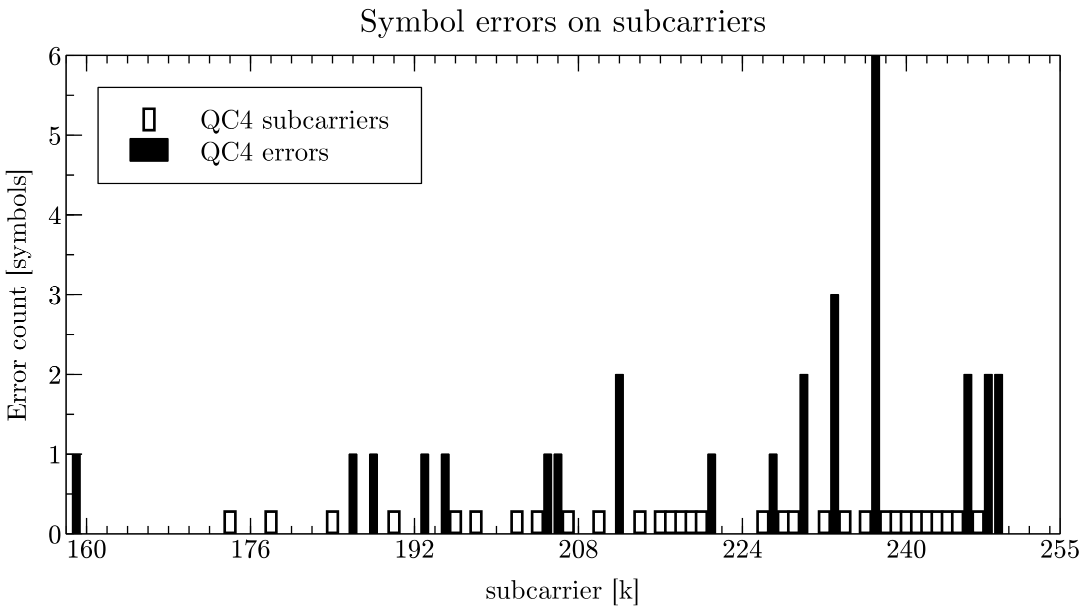

Figure 3.7: Transmission with QC4 STBC and selected subcarriers.

3.1.2 Method with the bitloading feedback

According to the MIMO STBC scheme application by the second method, the setup for a low SNR transmission and the Bitloading feedback algorithm (see Section 2.3.4) were established. DSL transmission parameters differs from the previous experiment in SNR and margin. Hence, the parameters set within this simulation are:

Signal to noise ratio .... SNR=14 dB
SNR gap .... $\Gamma = 8.8\,\mathrm{dB}$
Target error probability ...... $P_{eT} = 10^{-6}$
SNR margin .... $\gamma_m = 4\,\mathrm{dB}$
Channel bandwidth .... f=1.104 MHz
Subcarriers spacing .... $\Delta\mathrm{f} = 4312.5\,\mathrm{kHz}$
No. of available subcarriers... K=255
Bitloading .... RA waterfilling

Modeled channel and its frequency response are the same as in the previous experiment (Fig. 3.1), but the determined bitloading of the channel with the given configuration is different (Fig. 3.8). The bitloading graph is depicted in bits-per-dimension units and shows 0.5 bit/dimension (i.e.: 1 bit) channel loading for the majority of subcarriers. Further, there is depicted the un-rounded bitloading $\bar{b}_k$, the upper bound $\bar{b}_{\mathrm{UP}}$ and the lower bound $\bar{b}_{\mathrm{LOW}}$, which is used as decision within the Bitloading subcarriers selection algorithm. According to the selection algorithm and depicted bitloading, the subcarriers from index 169 are the target for the STBC application. Applied lower bound was $\bar{b}_{\mathrm{LOW}} = 0.153$ [bits/dimension] for the code with $Q = 2$ and $\bar{b}_{\mathrm{LOW}} = 0.144$ [bits/dimension] for the codes with $Q = 4$.

Achieved results of this experiment with 8 000 DMT symbols transferred are summarized in Table 3.2. Reference DSL transmission with disabled STBC functionality resulted in transfer of $\approx 10.1 \cdot 10^6$ bits and shown zero bit error rate. Consecutive columns in the table shows the resulting rate and BER for a different STBCs applied to the transmission. For example of the C2 code, the data rate increase was 26 % in comparison to the reference transmission. Note that this C2 code application was maintained within forty-three MIMO groups at total number of eighty-six subcarriers (see the bottommost row of the table).

Resulting values show the expected improvement in data rate increase, but the corresponding error results were not determined. With this observation another non-STBC transmission scheme – "Inserted ones", was incorporated. Subcarriers disabled by bitloading, but selected by the bitloading feedback algorithm, were re-enabled and set to carry one bit of information within the regular DSL transmission. Achieved data rate within this reference transmission with inserted ones was the highest of all presented and shown the bit error ratio: BER=$3.86 \cdot 10^{-6}$. Data rate increase was about 51 % in comparison to the reference transmission. All the eighty-seven subcarriers having the bitload value above the lower bound were utilized in this scheme. This scheme represents the highest bound where a maximal data rate is achieved with cost of the highest error rate. With these bound determined, it is suggested that the MIMO STBC application on the selected subcarriers considerably increases the initial non-STBC data rate with a limited error rate increase, which never exceeds the highest error rate given by the "Inserted ones" referential experiment.

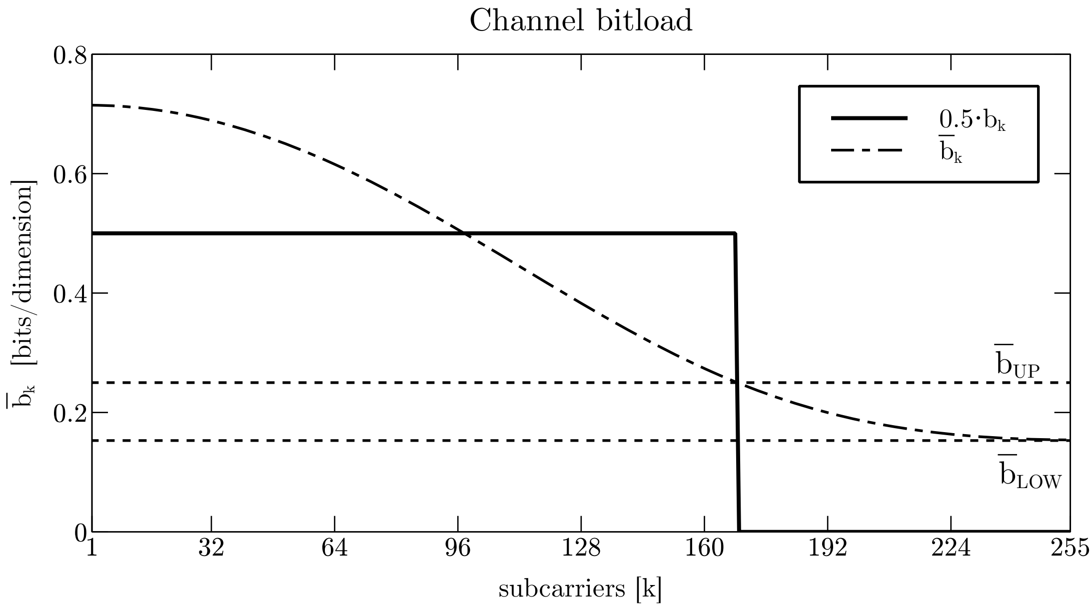

Figure 3.8: Bitloading of the selected channel model with upper and lower bounds.

Concept of this experiment was to utilize unused subcarriers, which were selected by a valid lower bitloading bound. To provide a valid lower bound, the SNR margin was applied within the tested system. In the consequence of this, the experiment did not shown desired error rate results with the MIMO STBC application, because the margin (SNR reserve) strongly decreased overall error rate below the target error probability level.

Table 3.2: Bitload feedback results for 8 000 DMT symbols transmitted.

	Reference	Inserted ones	C2	C3	C4	C4EP	QC4
Rate [10^6 bits]	10.1	15.3	12.7	11.4	11.0	11.0	11.3
Bits/symbol [bits]	1260	1913	1583	1423	1378	1378	1418
BER [-]	0	3.86E-06	0	0	0	0	0
Symbol Errors [symbols]	0	59	0	0	0	0	0
SER [-]	0	7.38E-03	0	0	0	0	0
No. of STBC subcarriers	0	87[*)]	86	87	84	84	84

Since the BER results presented in the Table 3.2 were zero valued, the only depicted experiment is the "Inserted ones" in Figure 3.9. Together with symbol errors, the utilized subcarriers are depicted too. The same subcarriers were selected either with the bitloading feedback algorithm and used in STBC application experiments presented also in the table of results.

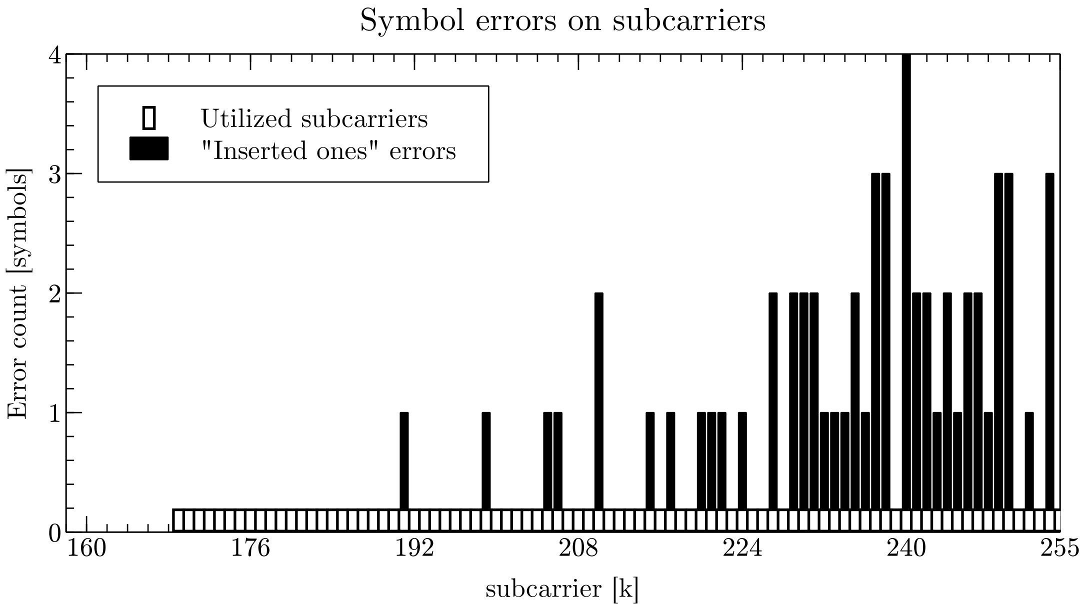

Figure 3.9: Transmission with inserted ones at selected subcarriers.

3.2 "Real channel" experiments

These experiments were performed to achieve results related to a "real" DSL system. The DSL channel was composed of direct and cross-talk channel responses, which were measured on real-world twisted pair cable (type: TCEPKPFLE). Additional channel impairments were induced by an additive white Gaussian noise (AWGN) and perfect synchronization at receiver were assumed. Opposite to the referential setup, the channel knowledge and the noise power spectral density were determined at receiver within initialization of DSL transmission with use of standardized ADSL training sequence. Since the twisted pair cable offers concrete multi-user channel, the multi-user functionality providing parallel simulations of the DSL transmission was incorporated in this setup.

The real TP cable of type TCEPKPFLE 25x4x0.4 consists of the 50 twisted pair wirelines and has length of 400 metres (1312 ft.). Frequency response measurements determined the attenuation and phase up to $\approx$ 35 MHz (i.e.: $\approx$ 8 000 subcarriers with spacing equal to 4.3125 kHz). For example of the first TP line, the frequency response magnitude of direct channel is depicted in Figure 3.10 and the magnitude of cross-talk channel to the second TP line is depicted in Figure 3.11. Corresponding impulse responses are depicted in Figure 3.12 and Figure 3.13 for the direct channel and cross-talk channel, respectively.

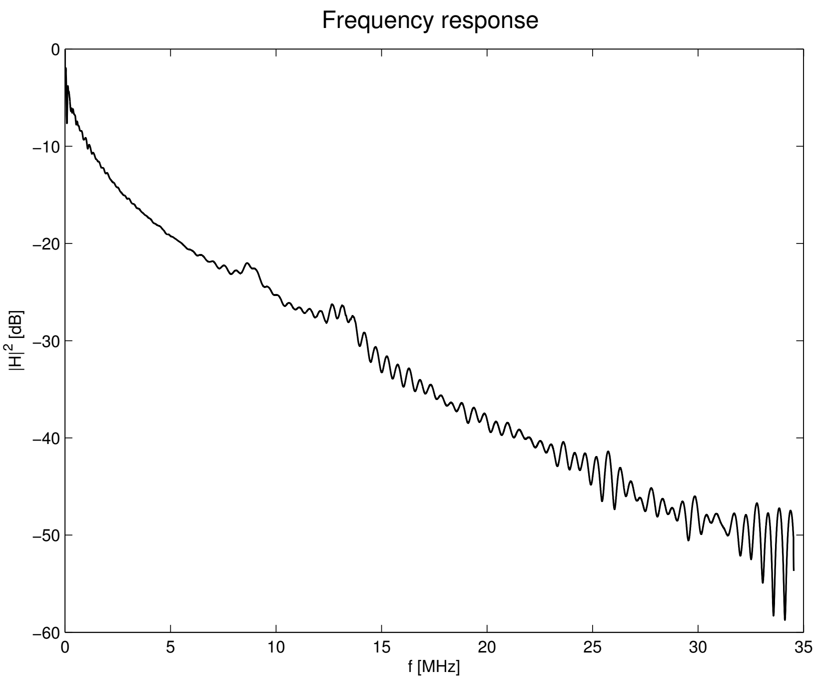

Figure 3.10: Frequency response magnitude of the first direct channel.

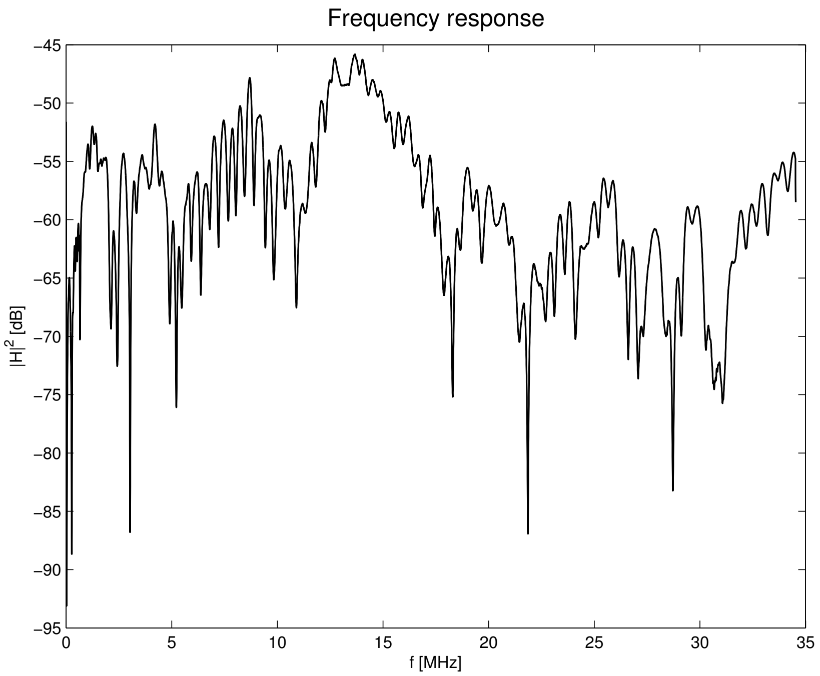

Figure 3.11: Frequency response magnitude of cross-talk channel from the first to the second TP line.

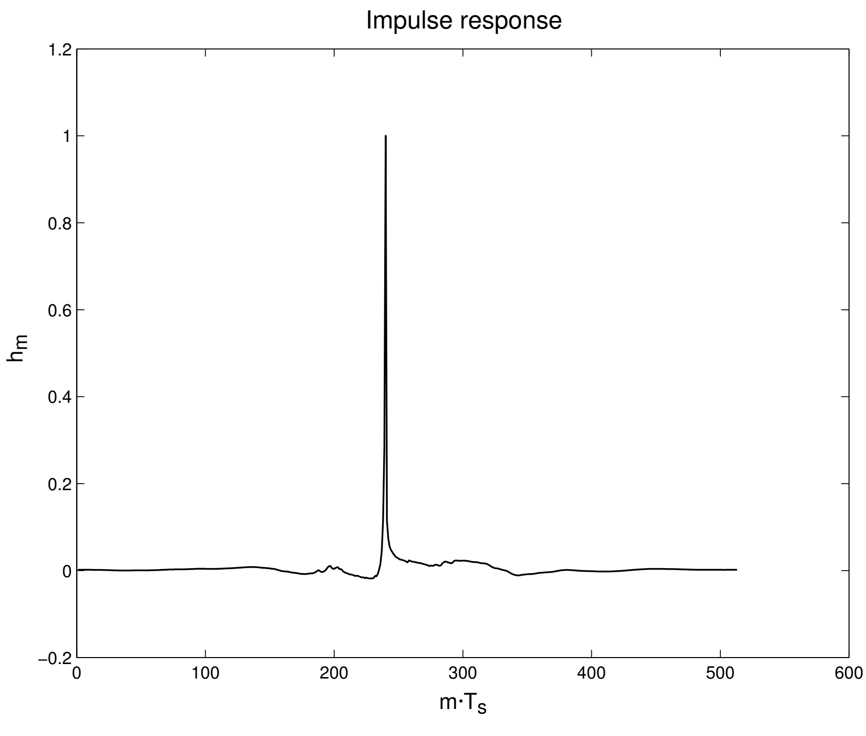

Figure 3.12: Impulse response of the first direct channel.

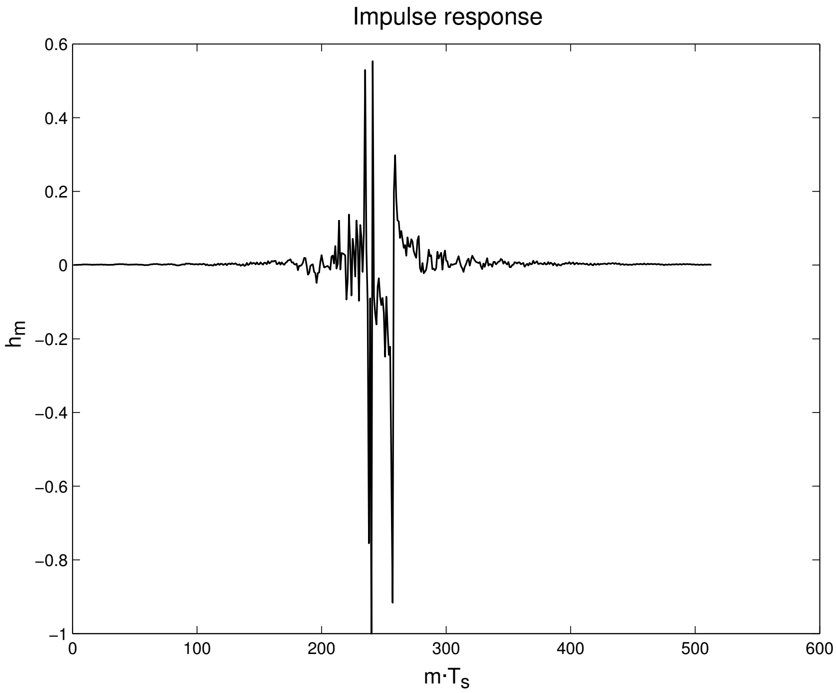

Figure 3.13: Impulse response of cross-talk channel from the first to the second TP line.

3.2.1 Method with the error feedback

According to the MIMO STBC scheme application by the first method, the setup for a high SNR transmission and the Error feedback algorithm (see Section 2.2.3) were established. Following DSL transmission parameters were set within the simulation:

Signal to noise ratio	SNR=12.5, 17.5, 25 and 50 dB
SNR gap	$\Gamma = 8.8\,\text{dB}$
Target error probability	$P_{eT} = 10^{-6}$
SNR margin	$\gamma_m = 4\,\text{dB}$
Channel bandwidth	f=1.104 MHz
Subcarriers spacing	$\Delta\text{f} = 4312.5\,\text{kHz}$
No. of available subcarriers	K=255
Bitloading	RA waterfilling
Channel estimation	yes
Noise PSD estimation	no
No. of simultaneous users	4
Channel topology	1) Independent single links (SISO)
	2) Multi-user (MIMO)

Both types of channel topology (single independent and multi-user with cross-talks) were evaluated within initial setup summarized in the above table. The Alamouti's STBC was initially applied. Achieved results of BER and data decrease for a four independent SISO channels are presented in Table 3.3. Further results of the same setup, but for multi-user channel model with cross-talks, achieved with Alamouti's STBC are presented in Table 3.4. Both tables show desired BER decrease of STBC application in comparison to each reference simulation without the STBC. In the case of MIMO channel, there is only a small difference of resulted BER decrease in comparison to SISO channel.

Results at low SNR show that the STBC application was not effective even with a large number of subcarriers utilizes. Moreover, the concrete BER values unpredictable increased. With this unpleasant observation, further simulations of other considered STBCs are not presented here and they were left for further research.

Table 3.3: Error feedback results for 2 000 DMT symbols transmitted – SISO.

User 1								
SNR	BER reference [-]	BER User1 [-]	BER decrease	Rate reference [bits]	Rate User1 [bits]	Rate decrease	No .of STBC sub-carriers	Symbol error threshold
12.5dB	4.72E-02	5.71E-02	121%	38100	37700	99.0%	4	91
17.5dB	9.80E-04	2.55E-04	26%	68400	67000	98.0%	18	4
25dB	2.11E-04	1.19E-04	56%	126100	124500	98.7%	26	2
50dB	5.47E-05	4.24E-05	78%	337400	313100	92.8%	36	2
User 2								
SNR	BER reference [-]	BER User2 [-]	BER decrease	Rate reference [bits]	Rate User2 [bits]	Rate decrease	No .of STBC sub-carriers	Symbol error threshold
12.5dB	4.58E-02	5.26E-02	115%	38100	37900	99.5%	4	88
17.5dB	9.38E-04	2.93E-04	31%	68400	67400	98.5%	14	4
25dB	2.26E-04	1.26E-04	56%	126100	125500	99.5%	22	2
50dB	5.51E-05	4.17E-05	76%	337500	310700	92.1%	36	2
User 3								
SNR	BER reference [-]	BER User3 [-]	BER decrease	Rate reference [bits]	Rate User3 [bits]	Rate decrease	No .of STBC sub-carriers	Symbol error threshold
12.5dB	6.56E-02	4.35E-02	66%	38200	38000	99.5%	6	126
17.5dB	9.68E-04	4.03E-04	42%	68500	67300	98.2%	16	4
25dB	1.83E-04	1.43E-04	78%	126100	124900	99.0%	20	2
50dB	5.46E-05	4.11E-05	75%	337400	310800	92.1%	34	2
User 4								
SNR	BER reference [-]	BER User4 [-]	BER decrease	Rate reference [bits]	Rate User4 [bits]	Rate decrease	No .of STBC sub-carriers	Symbol error threshold
12.5dB	4.71E-02	4.76E-02	101%	38200	37800	99.0%	4	91
17.5dB	9.83E-04	1.66E-04	17%	68600	67600	98.5%	18	4
25dB	3.02E-04	1.77E-04	59%	126100	124900	99.0%	24	3
50dB	5.47E-05	4.24E-05	78%	337600	312100	92.4%	34	2

Table 3.4: Error feedback results for 2 000 DMT symbols transmitted – MIMO.

User 1								
SNR	BER reference [-]	BER User1 [-]	BER decrease	Rate reference [bits]	Rate User1 [bits]	Rate decrease	No .of STBC sub-carriers	Symbol error threshold
12.5dB	5.34E-02	5.15E-02	96%	38400	37900	98.7%	8	104
17.5dB	9.55E-04	4.81E-04	50%	68500	67300	98.2%	12	4
25dB	2.11E-04	1.38E-04	65%	126300	124300	98.4%	30	2
50dB	5.23E-05	3.56E-05	68%	338400	311700	92.1%	40	2
User 2								
SNR	BER reference [-]	BER User2 [-]	BER decrease	Rate reference [bits]	Rate User2 [bits]	Rate decrease	No .of STBC sub-carriers	Symbol error threshold
12.5dB	6.30E-02	6.32E-02	100%	38100	38000	99.7%	2	121
17.5dB	2.34E-04	1.16E-04	50%	68500	66700	97.4%	18	2
25dB	9.13E-04	5.53E-04	61%	126200	124600	98.7%	30	7
50dB	5.05E-05	3.55E-05	70%	338200	310300	91.8%	42	2
User 3								
SNR	BER reference [-]	BER User3 [-]	BER decrease	Rate reference [bits]	Rate User3 [bits]	Rate decrease	No .of STBC sub-carriers	Symbol error threshold
12.5dB	4.66E-02	5.86E-02	126%	38600	38400	99.5%	2	91
17.5dB	2.27E-04	1.61E-04	71%	68800	67200	97.7%	16	2
25dB	9.76E-04	5.29E-04	54%	126300	124100	98.3%	30	7
50dB	4.93E-05	3.81E-05	77%	338300	314100	92.8%	36	2
User 4								
SNR	BER reference [-]	BER User4 [-]	BER decrease	Rate reference [bits]	Rate User4 [bits]	Rate decrease	No .of STBC sub-carriers	Symbol error threshold
12.5dB	5.89E-02	3.95E-02	67%	38200	38000	99.5%	8	113
17.5dB	9.66E-04	4.68E-04	48%	68900	67500	98.0%	14	4
25dB	2.25E-04	1.26E-04	56%	126200	124200	98.4%	30	2
50dB	4.79E-05	3.38E-05	71%	338600	313600	92.6%	38	2

3.2.2 Method with the bitloading feedback

According to the MIMO STBC scheme application by the second method, the setup for a low SNR transmission and the Bitloading feedback algorithm of the second variant (see Section 2.3.4) were established. Following DSL transmission parameters were set within this simulation are:

Signal to noise ratio	SNR=0 to 25 dB
SNR gap	$\Gamma = 8.8\,\mathrm{dB}$
Target error probability	$P_{eT} = 10^{-6}$
SNR margin	$\gamma_m = 4\,\mathrm{dB}$
Channel bandwidth	f=1.104 MHz and 8.832 MHz
Subcarriers spacing	Δf = 4312.5 kHz
No. of available subcarriers. . .	K=255 and 2047
Bitloading	RA waterfilling and LCRA discrete loading
Channel estimation	yes
Noise PSD estimation	none for SISO, enabled for MIMO
No. of simultaneous users	4
Channel topology	1) Independent single links (SISO)
. . .	2) Multi-user (MIMO)

The bitloading experiments were evaluated within combinations of following parameters: two types of channel topology (single independent and multi-user with cross-talks), two utilized bandwidths with 255 and 2047 subcarriers, two types of loading algorithms: Waterfilling RA and discrete loading LCRA. Further, all the STBC codes summarized in Appendix B were evaluated within these setup variants. Similarly to the referential experiment of bitloading feedback, the "Inserted ones" setups were incorporated in each "real channel" experiment.

Results of this extensive experiment are presented in graphs on the following pages. To describe the trade-offs between data rate and error rate, all characteristics were enumerated in percentage that was related to proper reference. The referential values for error ratios BER were the highest levels of error rate provided by "Inserted ones" setups within each experiment. Opposite to BER, the referential values for data rates were given by regular DSL transmission experiment provided initially for each of SNR, bitloading, bandwidth and channel's setup. Precise reference values and absolute values accomplished within these experiments are summarized in Appendix C.

Comparison of utilized STBCs for different channel topology, bitloading and utilized bandwidth setups is provided in Figures 3.14, 3.15, 3.16 and 3.17. Note that the M denotes the DMT size and $K = M/2 - 1$ is the number of available DMT subcarriers. The graphs, for example of Fig. 3.14 with $M = 512$, can be read as: the C2 code reduced the highest error rate level of "Inserted ones" transmission to 40 % at 0 dB SNR and its data rate boost was 650 % at 0 dB SNR in comparison to regular non-STBC transmission reference. The reason for this arrangement is that the applied SNR margin covered system's target error rate level in case of the regular non-STBC transmission reference.

Partial results achieved with different STBCs are depicted in Figures 3.18, 3.19 and 3.20 for SISO channel topology, RA waterfilling and 255 subcarriers setup; similarly Figures 3.21, 3.22

and 3.23 for MIMO channel topology, RA waterfilling and 255 subcarriers setup; Figures 3.24, 3.25 and 3.26 for SISO channel topology, RA waterfilling and 2047 subcarriers setup; and finally Figures 3.27, 3.28 and 3.29 for MIMO channel topology, RA waterfilling and 2047 subcarriers setup.

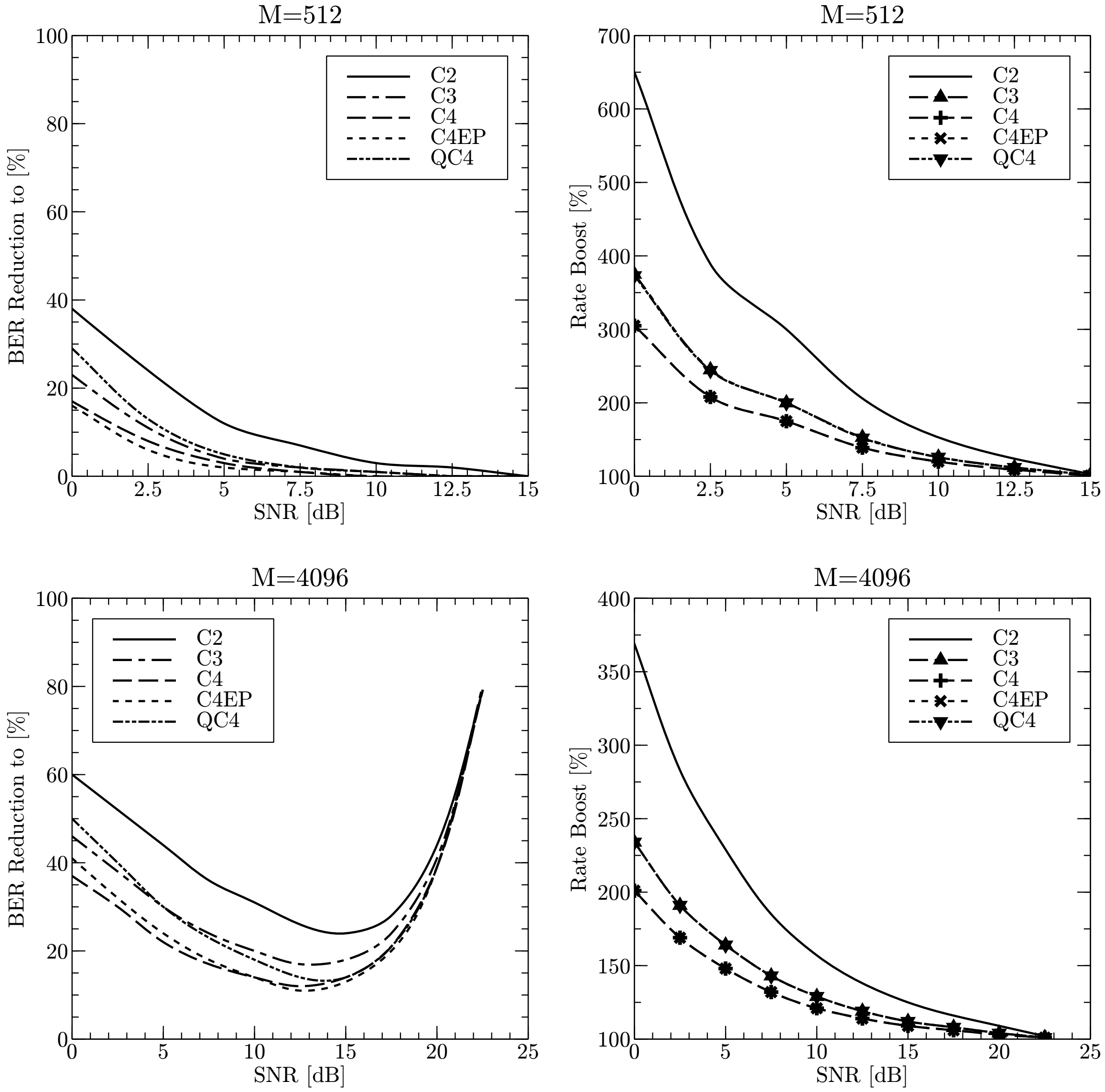

Figure 3.14: Comparison of STBC variants within SISO-RA setup and K=255 or 2047.

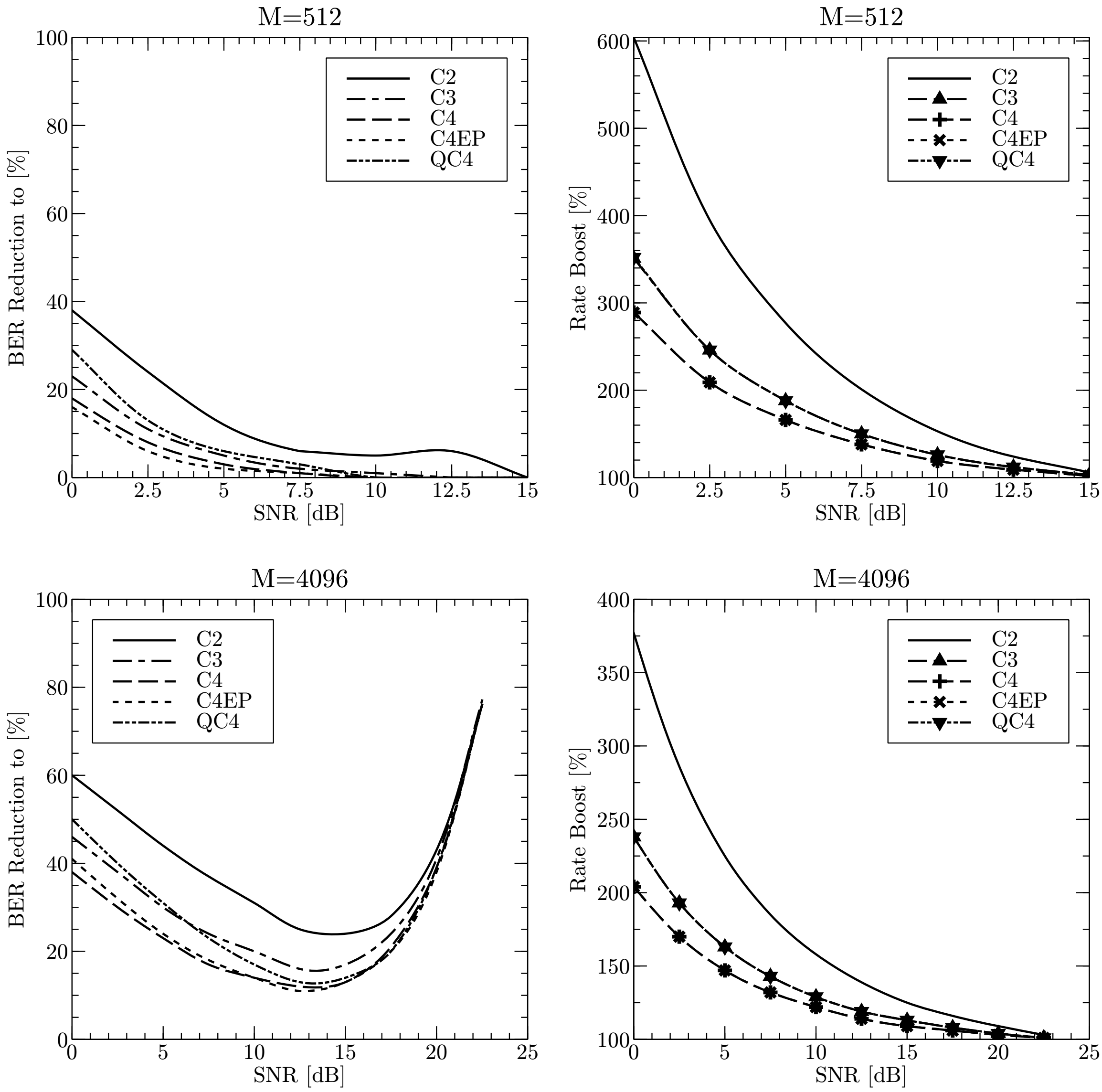

Figure 3.15: Comparison of STBC variants within SISO-LCRA setup and K=255 or 2047.

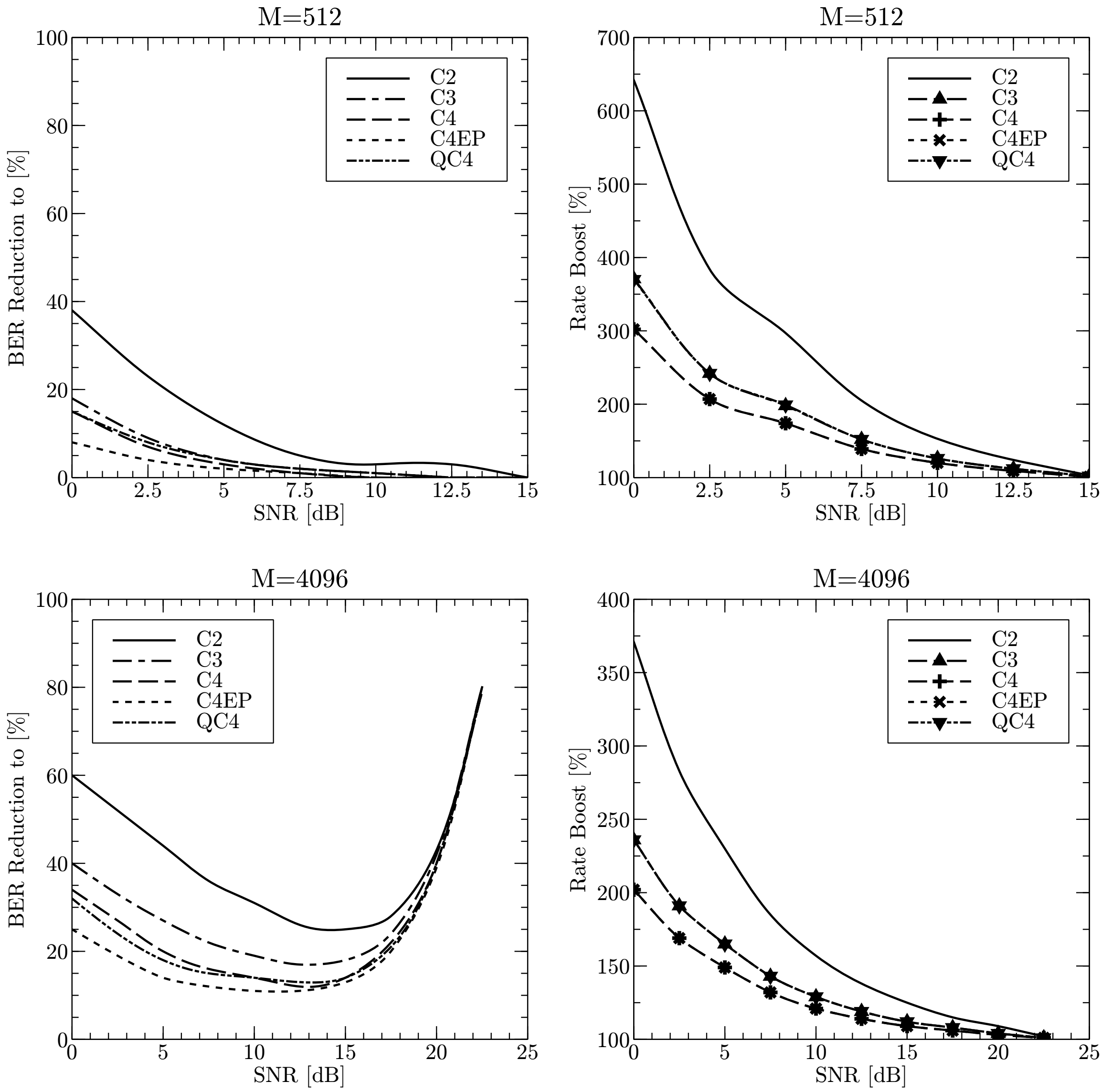

Figure 3.16: Comparison of STBC variants within MIMO-RA setup and K=255 or 2047.

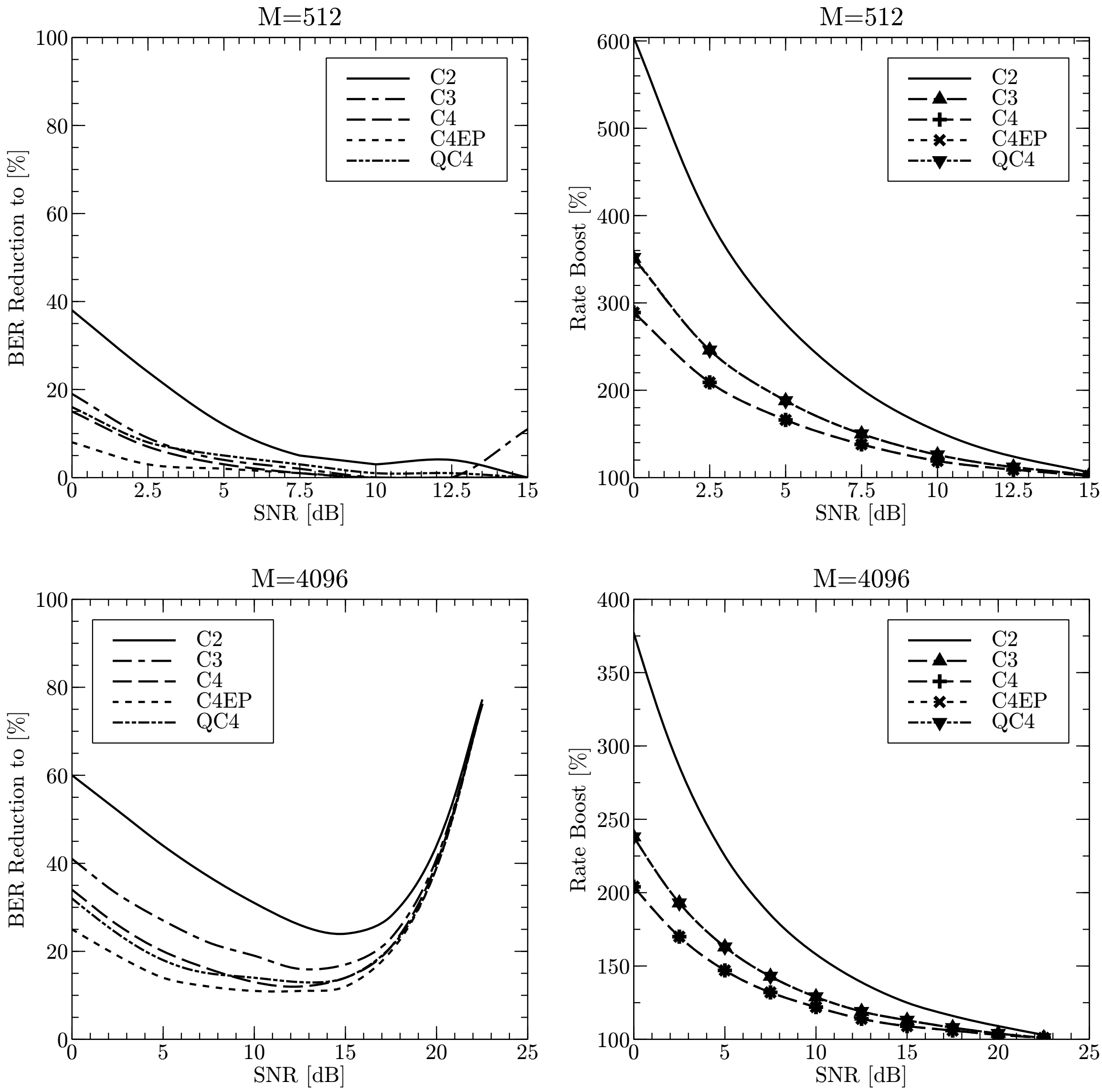

Figure 3.17: Comparison of STBC variants within MIMO-LCRA setup and K=255 or 2047.

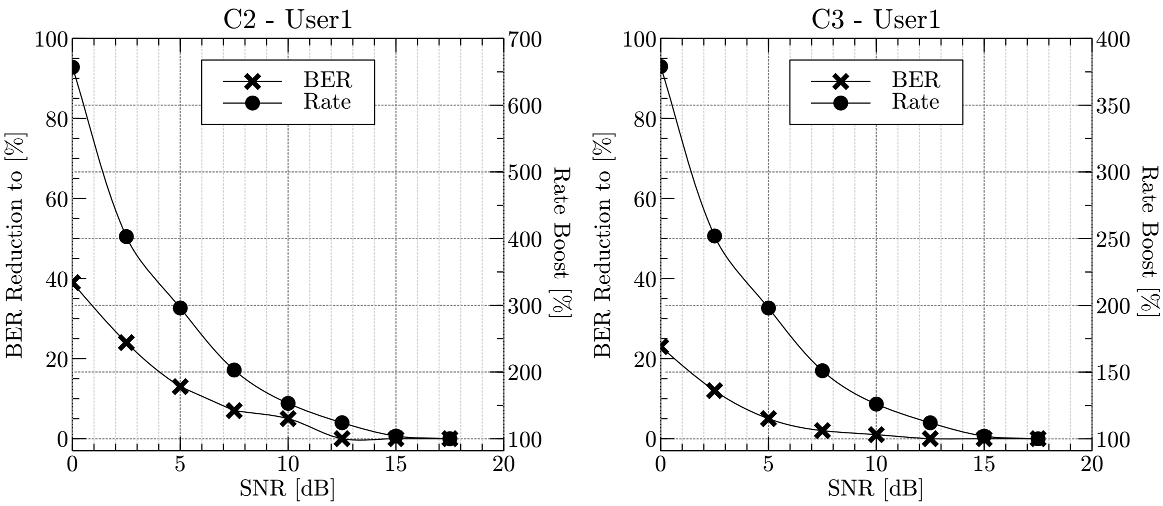

Figure 3.18: C2 and C3 STBCs results for User 1, K=255 and SISO-RA setup.

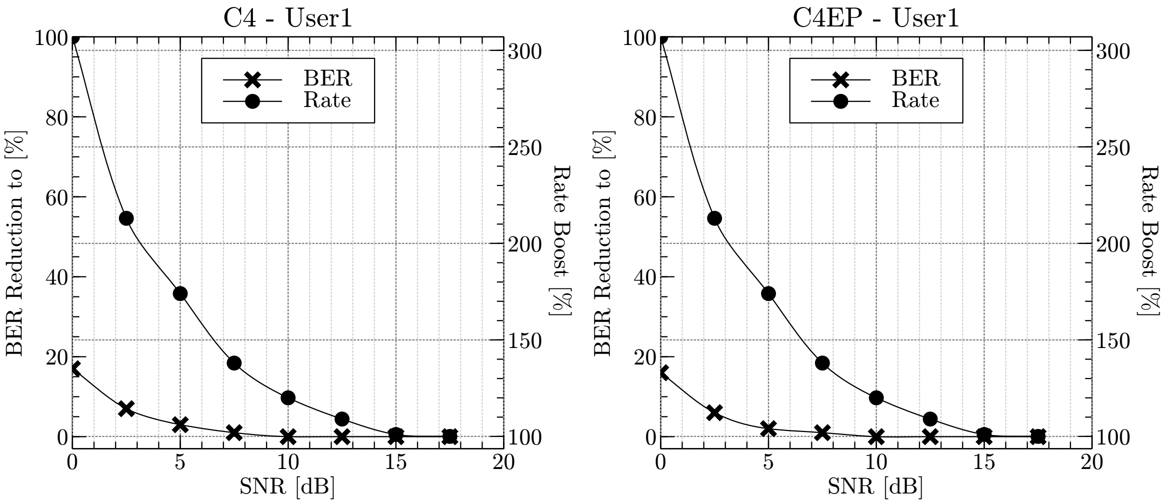

Figure 3.19: C4 and C4EP STBCs results for User 1, K=255 and SISO-RA setup.

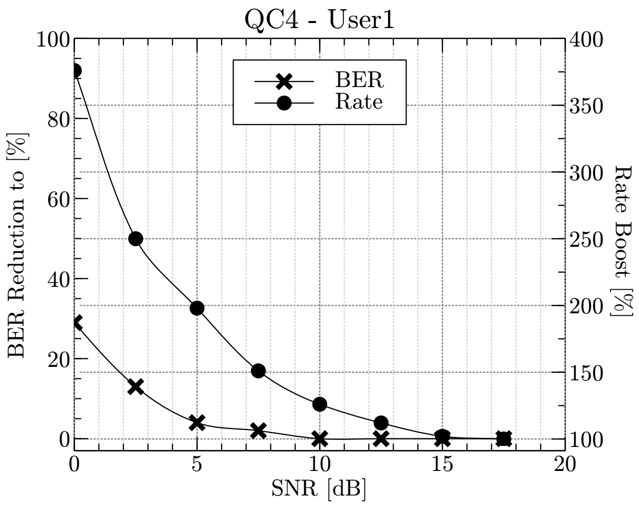

Figure 3.20: QC4 STBC results for User 1, K=255 and SISO-RA setup.

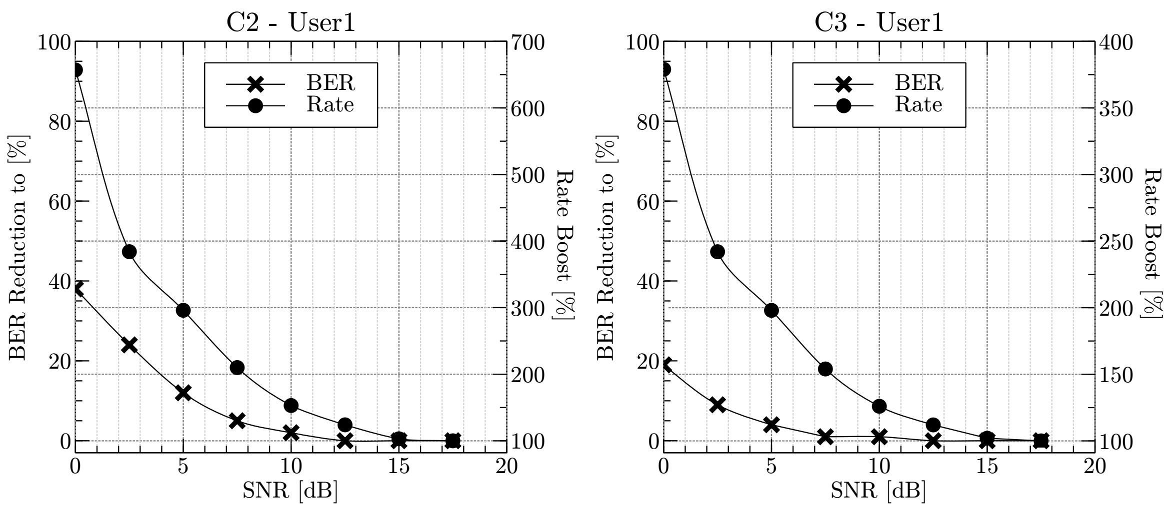

Figure 3.21: C2 and C3 STBCs results for User 1, K=255 and MIMO-RA setup.

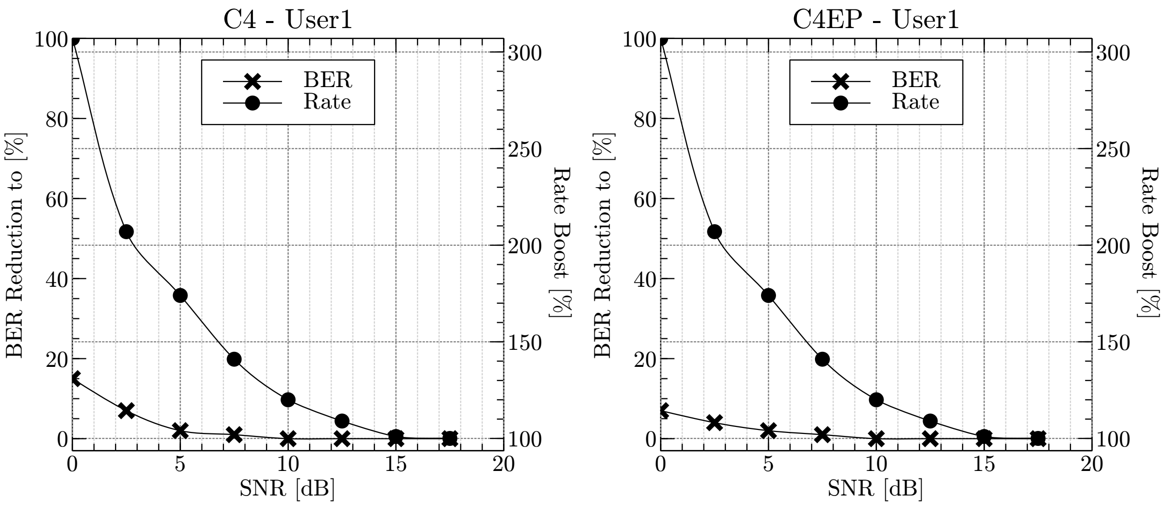

Figure 3.22: C4 and C4EP STBCs results for User 1, K=255 and MIMO-RA setup.

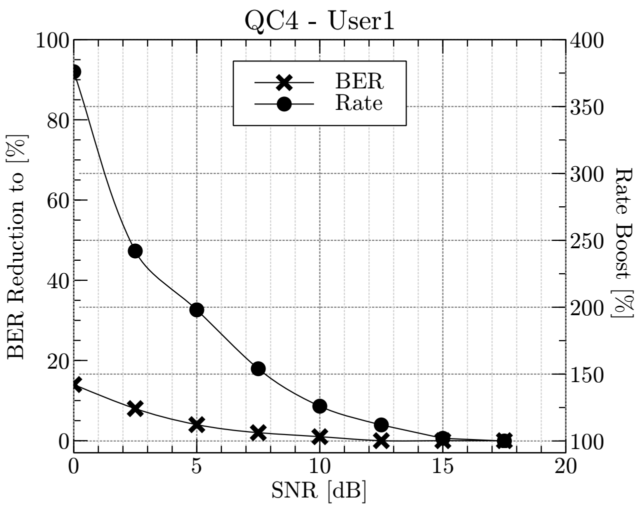

Figure 3.23: QC4 STBC results for User 1, K=255 and MIMO-RA setup.

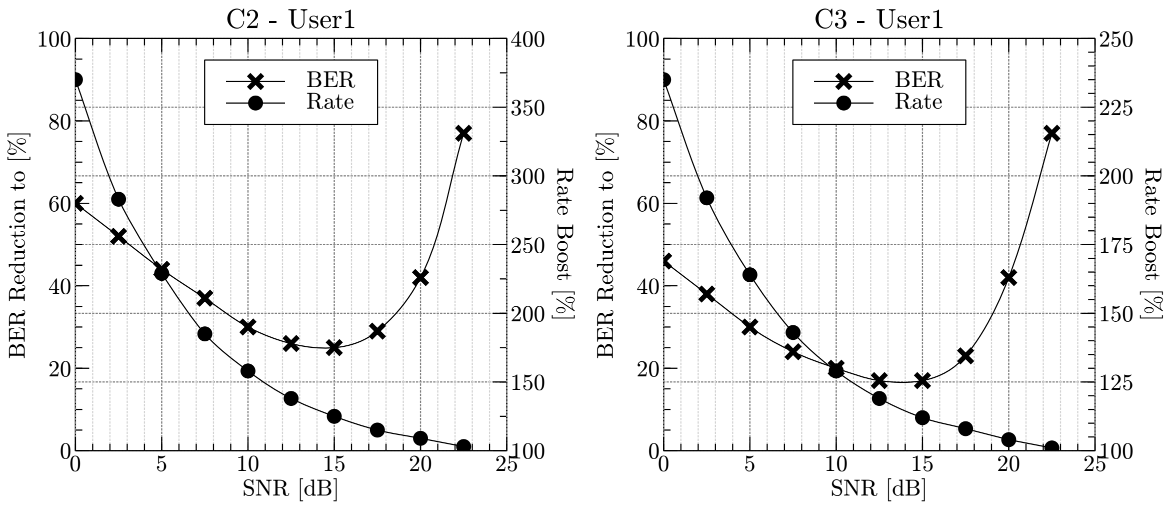

Figure 3.24: C2 and C3 STBCs results for User 1, K=2047 and SISO-RA setup.

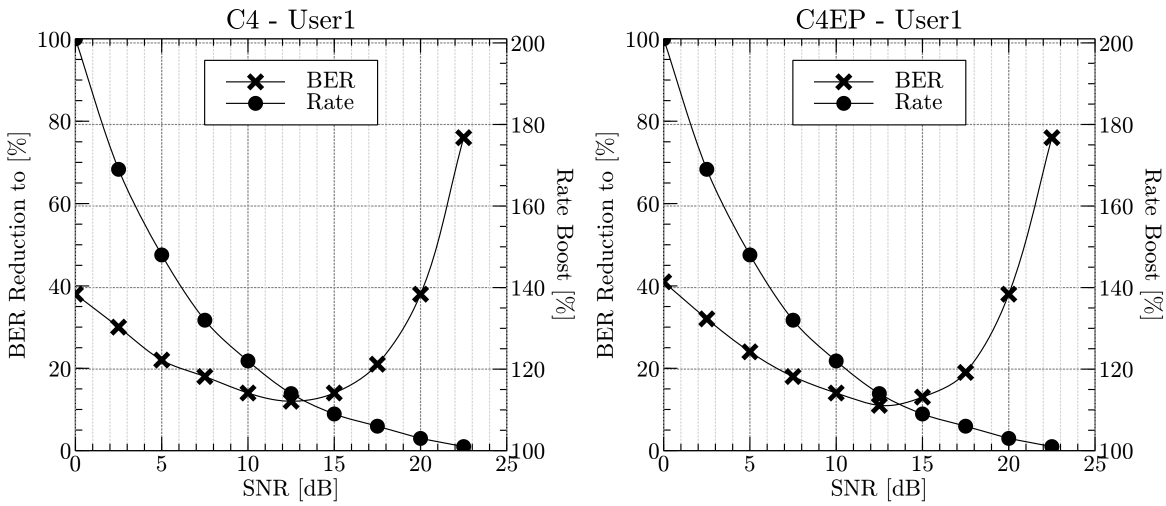

Figure 3.25: C4 and C4EP STBCs results for User 1, K=2047 and SISO-RA setup.

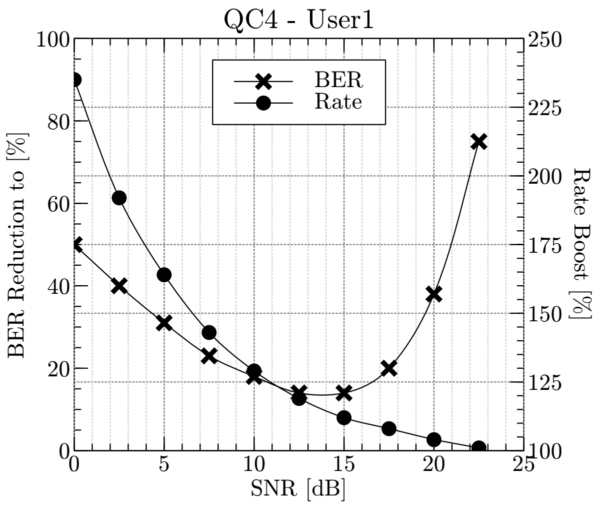

Figure 3.26: QC4 STBC results for User 1, K=2047 and SISO-RA setup.

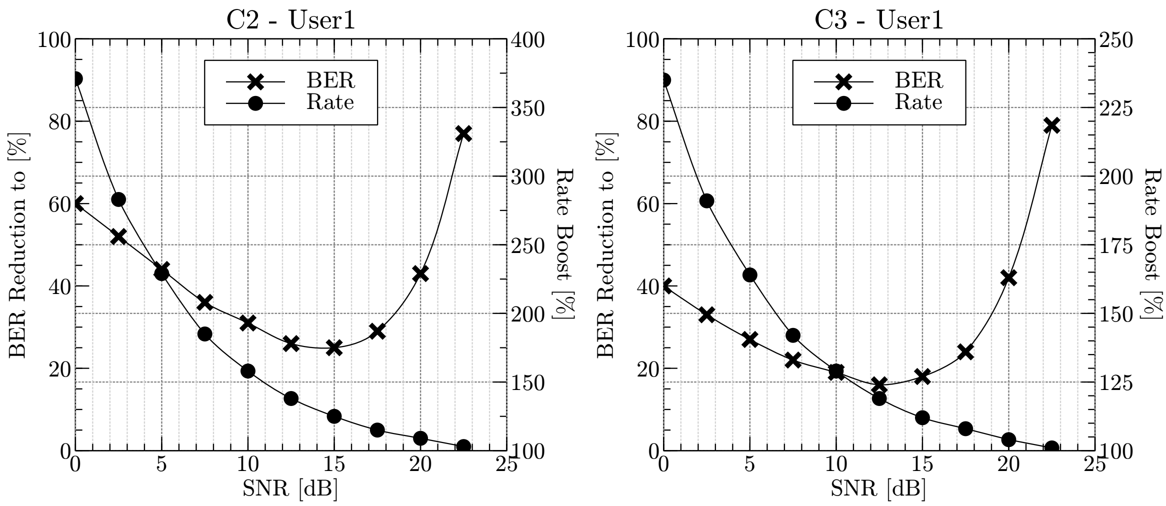

Figure 3.27: C2 and C3 STBCs results for User 1, K=2047 and MIMO-RA setup.

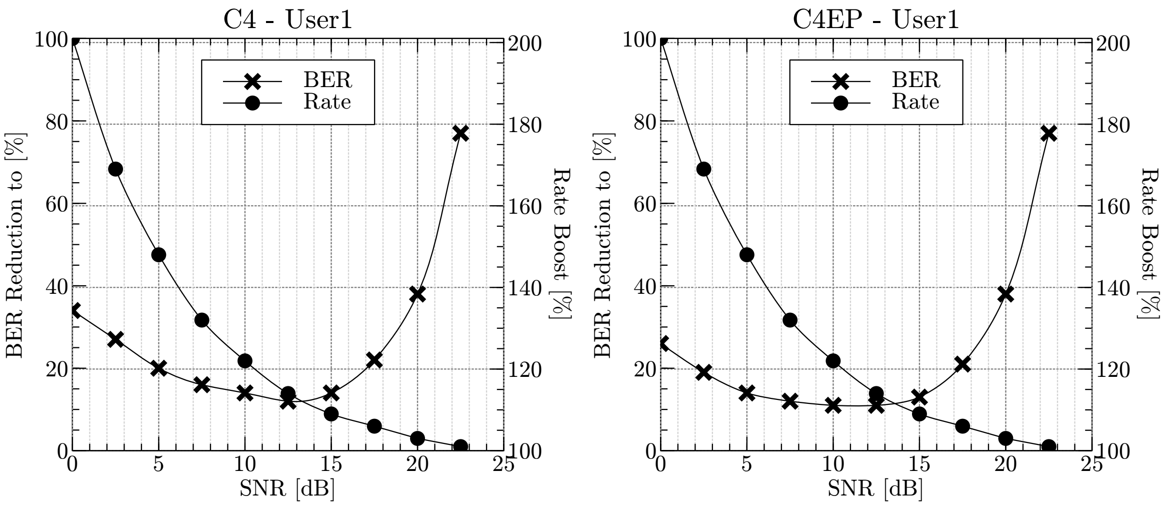

Figure 3.28: C4 and C4EP STBCs results for User 1, K=2047 and MIMO-RA setup.

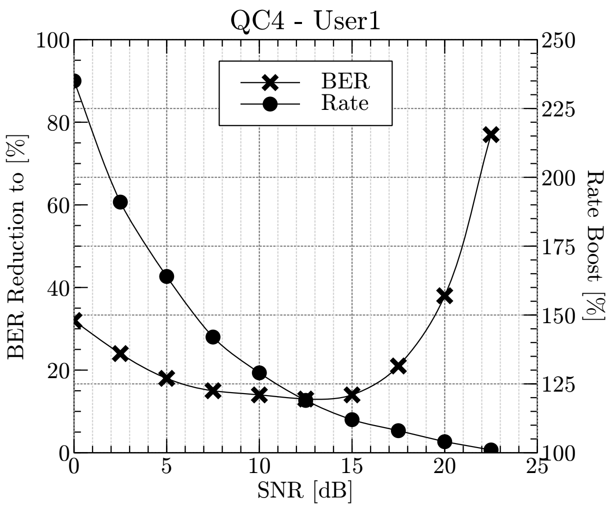

Figure 3.29: QC4 STBC results for User 1, K=2047 and MIMO-RA setup.

3.3 Conclusions

The experiments were performed using both referential setup utilizing the channel modeled by simple linear-phase FIR filter and the "real channel" setup utilizing the channel based on real measurements of DSL metallic cable.

The referential experiments for the first method, which applies the error feedback algorithm, proved the expectation of a significant error rate decrease using the proposed MIMO STBC scheme on the single DSL link transmission.

The referential experiments for the second method, which utilizes subcarriers disabled by regular bitloading algorithm, have shown the expected data rate increase. This method has also proven the validity of the bitloading lower bound for subcarrier selection with SNR margin. Due to the SNR margin strongly decrease overall error rate, the experiment did not achieved statistically valuable results (we have obtained zero error rate for 10^7 transmitted bits). Further experiments ("inserted ones"), which provided statistically valuable results with adequate amount of errors, have shown that the MIMO STBC application significantly increases the data rate at the cost of adequately small error rate increase. This increased error rate level was small enough and close to the system's target error probability.

The "real channel" error feedback experiments have shown significant error rate decrease at the cost of small data rate decrease for higher SNR cases. Evaluated setup has shown satisfying results, which supports theoretical expectations.

The bitloading feedback algorithm was heavily tested within the "real channel" experiments. The achieved results have confirmed validity of the proposed STBC application scheme with bitloading feedback algorithm in the second variant, which blindly utilizes all unused subcarriers. The application of STBC is always a trade-off between the higher data rate and the lower error rate. The data rate is always higher than that of original DSL and error rate is lower than the highest error rate of the full one-bit transmission on unused subcarriers.

Within this experiment setup, the LCRA algorithm for discrete loading was also evaluated. As the LCRA utilizes subcarrier information capacity in full range, the bitloading feedback results were expected to be flawed. The experiments shown that the LCRA does not affect the system performance of the bitloading feedback applied on a system with SNR margin.

Chapter 4

Conclusions

The main objectives of the thesis and the related research are to improve state-of-the-art techniques in the *digital subscriber line (DSL)* systems and to develop a novel method operating on telecommunication network physical layer of DSL systems. The new method is based on the application of the *multiple-input multiple-output (MIMO)* principles commonly used in todays wireless communication systems. It results in direct application of the new technique exploiting MIMO features in future implementations of the DSL physical layer.

Target DSL systems are the *very high speed digital subscriber lines (VDSL)* and the *asymmetric digital subscriber line (ADSL)* standardized by the International Telecommunication Union. Transmission media of these DSL technologies is copper-made wiring known as the *twisted pairs (TP)*.

In the first chapter, we introduced broadband access considerations and we figured out the motivation to keep the current DSL broadband technologies in progress. In the next chapter, we gave an introduction to basic concepts of DSL technology, set up the system model and gave a overall state of the art summary of enhanced DSL techniques. Further, we summarized the relevant MIMO concepts used in wireless systems.

In the fourth chapter, we proposed the scheme of MIMO STBC application on single DSL link and proposed two strategies to optimize the DSL transmission. Proposed scheme employs a MIMO view of the DMT subcarriers in frequency-time manner, which is in contrast with general space-time MIMO view known from wireless transmission systems. Adopted concept of information diversity provided by STBC that allows error performance improvement is not broken with application to DMT subcarriers with the assumptions that the subcarriers are independent and a non-alien FEXT is only present cross-talk.

Two methods, which apply proposed strategies, were presented. They provide the scheme setup by selection of DMT subcarriers for the STBC encoding. The first method directly targets the increase of error performance and the subcarriers selection is driven by subcarrier's error rate. Within this method, the subcarriers are STBC encoded in the case where their error rate exceeds a given threshold. The second method applies the STBC encoding on subcarriers, which were disabled by bitloading due to insufficient information capacity. The first method is applicable in general and the second is targeted to DSL channels with poor SNR conditions at a non-negligible number of subcarriers. Presented concept allows to be applied simultaneously to different users, but the cross-talks from users are not managed.

In the fifth chapter, we presented experimental results for referential channel model and for channel based on real measurements of DSL metallic cable – "real channel".

The referential experiments for the first method, which applies the error feedback algorithm, proved the expectation of a significant error rate decrease using the proposed MIMO STBC scheme on the single DSL link transmission.

The referential experiments for the second method, which utilizes subcarriers disabled by regular bitloading algorithm, have shown the expected data rate increase. This method has also proven the validity of the bitloading lower bound for subcarrier selection with SNR margin. Due to the SNR margin strongly decrease overall error rate, the experiment did not achieved statistically valuable results (we have obtained zero error rate for 10^7 transmitted bits). Further experiments ("inserted ones"), which provided statistically valuable results with adequate amount of errors, have shown that the MIMO STBC application significantly increases the data rate at the cost of adequately small error rate increase. This increased error rate level was small enough and close to the system's target error probability.

The "real channel" error feedback experiments have shown significant error rate decrease at the cost of small data rate decrease for higher SNR cases. Evaluated setup has shown satisfying results, which supports theoretical expectations.

The bitloading feedback algorithm was heavily tested within the "real channel" experiments. The achieved results have confirmed validity of the proposed STBC application scheme with bitloading feedback algorithm in the second variant, which blindly utilizes all unused subcarriers. The application of STBC is always a trade-off between the higher data rate and the lower error rate. The data rate is always higher than that of original DSL and error rate is lower than the highest error rate of the full one-bit transmission on unused subcarriers.

Within this experiment setup, the LCRA algorithm for discrete loading was also evaluated. As the LCRA utilizes subcarrier information capacity in full range, the bitloading feedback results were expected to be flawed. The experiments shown that the LCRA does not affect the system performance of the bitloading feedback applied on a system with SNR margin.

List of publications of Mr. Tomáš Mazanec

Journal papers

[A1] Mazanec T., Brothánek M. : FPGA implementace LMS a N-LMS algoritmu pro potlačeni akustického echa , Akustické listy vol.10, 4 (2004), p. 9-13 2004

Papers in proceedings

[B1] Mazanec T.,Heřmánek A., Kloub J. : Heterogeneous Platform for Stream Based Applications on FPGAs, accepted for: *Proceedings of the 21st International Conference on Field Programmable Logic and Applications – FPL 2011*, Chania, Crete, GREECE, 5.-7.9. 2011

[B2] Mazanec T.,Heřmánek A., Kamenický J. : Blind image deconvolution algorithm on NVIDIA CUDA platform, *Proceedings of the 13th IEEE Symposium on Design and Diagnostics of Electronic Circuits and Systems*, Vienna, AT, 14.-16.04.2010

[B3] Mazanec T.: Simulator of ADSL Physical Layer ,*Technical computing Prague 2007. 15th annual conference proceedings*, Praha, 14.11.2007

[B4] Mazanec Tomáš : Advanced Algorithms for Equalization on ADSL Channel , *Technical computing Prague 2006. 14th annual conference proceedings*, p. 68-75 , Prague, 26.10.2006

[B5] Mazanec T., Heřmánek A., Matoušek R.: Model of the transmission system of the reconnaissance system Orpheus , *Technical Computing Prague 2005 : 13th Annual Conference Proceedings*, p. 1-4 , Praha, 15.11.2005

Research reports

[C1] Mazanec T.: Použití MIMO technik pro xDSL, ÚTIA, Praha, Research Report 2305, 2011

[C2] Mazanec T., Heřmánek A. : ADSL - ekvalizační techniky, ÚTIA, Praha, Research Report 2184, 2007

[C3] Mazanec T., Heřmánek A.: Simulace ekvalizérů TEQ pro ADSL toolbox: výsledky experimentů, ÚTIA AV ČR, Praha, 2007, Research Report 2194

Software outputs and hardware prototypes

[D1] Mazanec T.: Application of CUDA in DSP: Implementation of FIR filter and Cross Ambiguity Function, 2009, software

[D2] Mazanec T., Kloub J., Heřmánek A. , Tichý M.: DVB-T2 Receiver Prototype: Physical Layer, 2009, prototype

[D3] Mazanec T. Heřmánek A. , Tichý M.: DVB-T2 Receiver: Physical Layer Simulator, 2009, software

[D4] Mazanec T., Kloub J., Heřmánek A.: HW Platform for Software Defined Radio, 2007, prototype

[D5] Mazanec T., Heřmánek A.: Matlab ADSL Toolbox ver. 11, 2007, software

[D6] Mazanec T., Heřmánek A.: Simulace ADSL downstream přenosu Webová aplikace, ÚTIA AV ČR, Praha, 2007, software

[D7] Mazanec T., Heřmánek A.: Simulátor fyzické vrstvy ADSL modemu, ÚTIA AV ČR, Praha, 2007, software

Chapter 5

Acknowledgements

This report was supported by project SCALOPES No.: Artemis JU 100029, MSMT 7H09005.

Appendix A

Selected mathematical definitions

A.1 DFT matrix

Let α be a primitive M-th root unity, i.e.: $\alpha = e^{-j2\pi/M}$, then the *M-point discrete Fourier (DFT) matrix* is defined as:

$$\mathcal{F}_M = \begin{bmatrix} 1 & 1 & 1 & \dots & 1 \\ 1 & \alpha & \alpha^2 & \dots & \alpha^{M-1} \\ 1 & \alpha^2 & \alpha^4 & & \alpha^{2(M-1)} \\ \vdots & \vdots & & \ddots & \vdots \\ 1 & \alpha^{M-1} & \alpha^{2(M-1)} & \dots & \alpha^{(M-1)(M-1)} \end{bmatrix} \tag{A.1}$$

The corresponding *M-point inverse DFT matrix* is given by: $\mathcal{I}_M = \frac{\mathcal{F}_M^{\mathrm{H}}}{M}$, such that $\mathcal{F}_M \mathcal{I}_M = \mathbf{I}_M$, where $\mathbf{I}_M$ denotes the $M \times M$ identity matrix. Notice that $\mathcal{F}_M$ and $\mathcal{I}_M$ are symmetric.

A.2 QR matrix decomposition

The *QR-decomposition* of a matrix $\mathbf{A} \in \mathbb{C}^{M \times N}$ (with $M \geq N$) is defined as:

$$\mathbf{A} = \mathbf{QR} \tag{A.2}$$

where $\mathbf{Q}$ is an $M \times N$ unitary matrix ($\mathbf{QQ}^{\mathrm{H}} = \mathbf{Q}^{\mathrm{H}}\mathbf{Q} = \mathbf{I}$) and $\mathbf{R}$ is an $N \times N$ upper triangular matrix.

A.3 Singular value decomposition (SVD)

Every $M \times N$ matrix $\mathbf{A} \in \mathbb{C}^{M \times N}$ (with $M \geq N$) can be decomposed as:

$$\mathbf{A} = \mathbf{U\Lambda V}^{\mathrm{H}} \tag{A.3}$$

where $\mathbf{U} \in \mathbb{C}^{M \times M}$ and $\mathbf{V} \in \mathbb{C}^{N \times N}$ are unitary matrices, $\mathbf{UU}^{\mathrm{H}} = \mathbf{U}^{\mathrm{H}}\mathbf{U} = \mathbf{I}$ and $\mathbf{VV}^{\mathrm{H}} = \mathbf{U}^{\mathrm{H}}\mathbf{V} = \mathbf{I}$, containing the left singular vectors $\mathbf{u}_i$ and the right singular vectors $\mathbf{v}_i$, respectively. The matrix $\mathbf{\Lambda} \in \mathbb{R}^{M \times N}$ is real, non-negative and diagonal with its diagonal elements arranged in non-increasing order, i.e.: $\mathbf{\Lambda} = \mathrm{diag}\{\sqrt{\lambda_1}, \sqrt{\lambda_2}, \dots, \sqrt{\lambda_M}\}$ such that $\lambda_1 \geq \lambda_2 \geq \dots \geq \lambda_M \geq 0$. If the matrix $\mathbf{A}$ has a rank $R < M$, then $M - R$ singular values are equal to zero.
The columns of $\mathbf{U}$ are orthonormal eigenvectors of $\mathbf{AA}^{\mathrm{H}}$, the columns of $\mathbf{V}$ are orthonormal eigenvectors of $\mathbf{A}^{\mathrm{H}}\mathbf{A}$ and $\lambda_1, \lambda_2, \dots, \lambda_M$ are the eigenvalues of $\mathbf{AA}^{\mathrm{H}}$.

A.4 Complementary error function

Complementary error function $\text{erfc}(x)$ is the probability that a zero-mean Gaussian random variable with the variance $\sigma^2 = 0.5$ exceeds the value x in the argument and it is given by:

$$\text{erfc}(x) = \frac{2}{\sqrt{\pi}} \int_x^\infty e^{-t^2} \mathrm{d}t \tag{A.4}$$

It equals to twice integral of a normalized Gaussian function between x and infinity.

A.5 Q function

The $\mathcal{Q}$ function is used to evaluate probability error in digital communication. It is the integral of a zero-mean unit-variance Gaussian random variable from some specified argument to infinity:

$$\mathcal{Q}(x) = \frac{1}{\sqrt{2\pi}} \int_x^\infty e^{-\frac{t^2}{2}} \mathrm{d}t \tag{A.5}$$

It is related to the complementary error function (A.4) as:

$$\mathcal{Q}(x) = \frac{1}{2}\text{erfc}\left(\frac{x}{\sqrt{2}}\right) \tag{A.6}$$

Appendix B

STBC matrices

For a given space-time block coding (STBC) matrix: the elements $\mathbb{X}_p$ denote transmitted complex symbols, each column belongs to a specific antenna and matrix rows represent consecutive symbols transmitted in time within one STBC block.

B.1 Alamouti's STBC

According to Alamouti's proposition in [1], the STBC for a two antenna MIMO system can be described by the following matrix:

$$\mathbf{C}_2 = \begin{bmatrix} \mathbb{X}_1 & \mathbb{X}_2 \\ -\mathbb{X}_2^* & \mathbb{X}_1^* \end{bmatrix} \tag{B.1}$$

B.2 Tarokh et.al. STBCs

Tarokh et.al. in [41] generalized Alamouti's STBC for a multi-antenna systems. Tarokh's three and four antenna STBCs $\mathbf{C}_3$ and $\mathbf{C}_4$ can be defined as (B.2) and (B.2), respectively.

$$\mathbf{C}_3 = \begin{bmatrix} \mathbb{X}_1 & \mathbb{X}_2 & \frac{1}{\sqrt{2}}\mathbb{X}_3 \\ -\mathbb{X}_2^* & \mathbb{X}_1^* & \frac{1}{\sqrt{2}}\mathbb{X}_3 \\ \frac{1}{\sqrt{2}}\mathbb{X}_3^* & \frac{1}{\sqrt{2}}\mathbb{X}_3^* & -\frac{1}{2}(\mathbb{X}_1 + \mathbb{X}_1^* - \mathbb{X}_2 + \mathbb{X}_2^*) \\ \frac{1}{\sqrt{2}}\mathbb{X}_3^* & -\frac{1}{\sqrt{2}}\mathbb{X}_3^* & \frac{1}{2}(\mathbb{X}_1 - \mathbb{X}_1^* + \mathbb{X}_2 + \mathbb{X}_2^*) \end{bmatrix} \tag{B.2}$$

$$\mathbf{C}_4 = \begin{bmatrix} \mathbb{X}_1 & \mathbb{X}_2 & \frac{1}{\sqrt{2}}\mathbb{X}_3 & \frac{1}{\sqrt{2}}\mathbb{X}_3 \\ -\mathbb{X}_2^* & \mathbb{X}_1^* & \frac{1}{\sqrt{2}}\mathbb{X}_3 & -\frac{1}{\sqrt{2}}\mathbb{X}_3 \\ \frac{1}{\sqrt{2}}\mathbb{X}_3^* & \frac{1}{\sqrt{2}}\mathbb{X}_3^* & -\frac{1}{2}(\mathbb{X}_1 + \mathbb{X}_1^* - \mathbb{X}_2 + \mathbb{X}_2^*) & \frac{1}{2}(\mathbb{X}_1 - \mathbb{X}_1^* - \mathbb{X}_2 - \mathbb{X}_2^*) \\ \frac{1}{\sqrt{2}}\mathbb{X}_3^* & -\frac{1}{\sqrt{2}}\mathbb{X}_3^* & \frac{1}{2}(\mathbb{X}_1 - \mathbb{X}_1^* + \mathbb{X}_2 + \mathbb{X}_2^*) & -\frac{1}{2}(\mathbb{X}_1 + \mathbb{X}_1^* + \mathbb{X}_2 - \mathbb{X}_2^*) \end{bmatrix} \tag{B.3}$$

B.3 Other STBCs

B.3.1 Quasi-orthogonal STBC variant

Jafarkhani in [33] proposed a quasi-orthogonal space-time block codes (QOSTBC) achieving the code-rate equal to one. Selected four antenna QOSTBC can be defined as:

$$\mathbf{C}_{\mathrm{Q4}} = \begin{bmatrix} \mathbb{X}_1 & \mathbb{X}_2 & \mathbb{X}_3 & \mathbb{X}_4 \\ -\mathbb{X}_2^* & \mathbb{X}_1^* & -\mathbb{X}_4^* & \mathbb{X}_3^* \\ -\mathbb{X}_3^* & -\mathbb{X}_4^* & \mathbb{X}_1^* & \mathbb{X}_2^* \\ \mathbb{X}_4 & -\mathbb{X}_3 & -\mathbb{X}_2 & \mathbb{X}_1 \end{bmatrix} \tag{B.4}$$

B.3.2 Equal power optimized STBC

Ganesan in [17] proposed STBC multi-antenna schemes that keep even power levels over the transmitted symbols. Selected four antenna equal-power STBC can be defined as:

$$\mathbf{C}_{\mathrm{4EP}} = \begin{bmatrix} \mathbb{X}_1 & \mathbb{X}_2 & \mathbb{X}_3 & 0 \\ -\mathbb{X}_2^* & \mathbb{X}_1^* & 0 & \mathbb{X}_3 \\ -\mathbb{X}_3^* & 0 & \mathbb{X}_1^* & -\mathbb{X}_2 \\ 0 & -\mathbb{X}_3^* & \mathbb{X}_2^* & \mathbb{X}_1 \end{bmatrix} \tag{B.5}$$

Appendix C

”Real channel” experiments results

Legend for the Tables:
rate0 – reference data rate, unused subcarriers have bk=0
rate1 – data rate with ”inserted ones” reference, unused subcarriers have bk=1
rateSTC2 – data rate with Alamouti’s STBC - C2 applied and unused subcarriers have bk=1
rateSTC3 – dtto, STBC - C3
rateSTC4 – dtto, STBC - C4
rateSTC4EP – dtto, Equal-power STBC - C4
rateSTQC4 – dtto, Quasi-orthogonal STBC - C4
err- prefix means erroneous bits count
ber- prefix means bit error ratio

SISO-RA-User1-N512

SNR	rate0	err0	rate1	err1	rateSTC2	errSTC2	rateSTC3	errSTC3	rateSTC4	errSTC4	rateSTC4EP	errSTC4EP	rateSTQC4	errSTQC4	SST
0	84000	0	1020000	95846	552000	20129	318000	6917	258000	4232	258000	3788	316000	8642	234
2.5	144000	0	1020000	44763	580000	6010	363000	1834	306000	997	306000	757	360000	2005	218
5	212000	1	1044000	14667	628000	1117	419000	269	368000	154	368000	88	420000	262	208
7.5	344000	0	1060000	2695	700000	122	521000	25	476000	14	476000	15	520000	26	178
10	536000	0	1108000	268	820000	10	677000	2	641000	0	641000	0	676000	0	142
12.5	804000	0	1196000	26	1000000	0	900000	0	876000	0	876000	0	900000	0	98
15	1252000	0	1344000	6	1296000	0	1273000	0	1267000	0	1267000	0	1272000	0	22
17.5	1732000	1	1736000	2	1732000	0	1732000	0	1732000	0	1732000	0	1732000	0	0
20	2372000	7	2376000	10	2372000	4	2372000	7	2372000	6	2372000	9	2372000	3	0
22.5	3016000	44	3016000	49	3016000	49	3016000	66	3016000	68	3016000	49	3016000	47	0
25	3780000	238	3780000	236	3780000	284	3780000	228	3780000	251	3780000	247	3780000	209	0

SNR	ber0	ber1	berST-C2	berST-C3	berST-C4	berST-C4EP	berST-QC4
0	0	9.4E-02	3.6E-02	2.2E-02	1.6E-02	1.5E-02	2.7E-02
2.5	0	4.4E-02	1.0E-02	5.1E-03	3.3E-03	2.5E-03	5.6E-03
5	0	1.4E-02	1.8E-03	6.4E-04	4.2E-04	2.4E-04	6.2E-04
7.5	0	2.5E-03	1.7E-04	4.8E-05	2.9E-05	3.2E-05	5.0E-05
10	0	2.4E-04	1.2E-05	3.0E-06	0	0	0
12.5	0	2.2E-05	0	0	0	0	0
15	0	4.5E-06	0	0	0	0	0
17.5	5.77E-07	1.2E-06	0	0	0	0	0
20	2.95E-06	4.2E-06	1.7E-06	3.0E-06	2.5E-06	3.8E-06	1.3E-06
22.5	1.46E-05	1.6E-05	1.6E-05	2.2E-05	2.3E-05	1.6E-05	1.6E-05
25	6.30E-05	6.2E-05	7.5E-05	6.0E-05	6.6E-05	6.5E-05	5.5E-05

SNR	Rate1 vs. Rate0	RateST-C2 vs. Rate0	RateST-C3 vs. Rate0	RateST-C4 vs. Rate0	RateST-C4EP vs. Rate0	RateST-QC4 vs. Rate0
0	1214%	657%	379%	307%	307%	376%
2.5	708%	403%	252%	213%	213%	250%
5	492%	296%	198%	174%	174%	198%
7.5	308%	203%	151%	138%	138%	151%
10	207%	153%	126%	120%	120%	126%
12.5	149%	124%	112%	109%	109%	112%
15	107%	104%	102%	101%	101%	102%
17.5	100%	100%	100%	100%	100%	100%
20	100%	100%	100%	100%	100%	100%
22.5	100%	100%	100%	100%	100%	100%
25	100%	100%	100%	100%	100%	100%

SNR	Ber1 reference	BerST-C2 vs. Ber1	BerST-C3 vs. Ber1	BerST-C4 vs. Ber1	BerST-C4EP vs. Ber1	BerST-QC4 vs. Ber1
0	100%	39%	23%	17%	16%	29%
2.5	100%	24%	12%	7%	6%	13%
5	100%	13%	5%	3%	2%	4%
7.5	100%	7%	2%	1%	1%	2%
10	100%	5%	1%	0%	0%	0%
12.5	100%	0%	0%	0%	0%	0%
15	100%	0%	0%	0%	0%	0%
17.5	100%	0%	0%	0%	0%	0%
20	100%	40%	70%	60%	90%	30%
22.5	100%	100%	135%	139%	100%	96%
25	100%	120%	97%	106%	105%	89%

Figure C.1: SISO-RA-User1-N512 experiment setup

SISO-RA-User1-N4096

SNR	rate0	err0	rate1	err1	rateSTC2	errSTC2	rateSTC3	errSTC3	rateSTC4	errSTC4	rateSTC4EP	errSTC4EP	rateSTQC4	errSTQC4	SST
0	167500	244	1071500	199067	619500	69359	393250	33400	337000	23527	337000	25726	393500	36868	1808
2.5	237500	284	1109000	161687	673000	51256	455375	24964	400625	17269	400625	18625	455000	26498	1742
5	322000	255	1150500	122114	736000	34143	529000	16770	477250	11209	477250	11988	529000	17231	1656
7.5	455500	455	1232000	95001	843500	23749	649375	12123	601000	8245	601000	8552	649500	11398	1552
10	621000	773	1336500	73556	978500	16405	799875	8742	754875	5894	754875	6014	799500	7800	1430
12.5	834000	1292	1469000	53668	1151500	10778	992625	6149	952875	4139	952875	3892	992500	5047	1270
15	1097000	2215	1641500	40475	1369000	8318	1233125	5234	1199000	4140	1199000	3788	1233000	4212	1088
17.5	1425500	4151	1864500	30258	1645000	7626	1535000	5842	1507625	5045	1507625	4730	1535000	5003	878
20	1819000	7357	2136500	23093	1977500	8924	1898125	8521	1878250	7669	1878250	7759	1898000	7763	634
22.5	2354500	14464	2482500	19888	2418500	14830	2386375	14716	2378500	14557	2378500	14556	2386500	14428	256
25	2953500	25764	2954000	25670	2953500	25391	2953500	25596	2953500	25503	2953500	25385	2953500	25508	0

SNR	ber0	ber1	berST-C2	berST-C3	berST-C4	berST-C4EP	berST-QC4
0	1.5E-03	1.9E-01	1.1E-01	8.5E-02	7.0E-02	7.6E-02	9.4E-02
2.5	1.2E-03	1.5E-01	7.6E-02	5.5E-02	4.3E-02	4.6E-02	5.8E-02
5	7.9E-04	1.1E-01	4.6E-02	3.2E-02	2.3E-02	2.5E-02	3.3E-02
7.5	1.0E-03	7.7E-02	2.8E-02	1.9E-02	1.4E-02	1.4E-02	1.8E-02
10	1.2E-03	5.5E-02	1.7E-02	1.1E-02	7.8E-03	8.0E-03	9.8E-03
12.5	1.5E-03	3.7E-02	9.4E-03	6.2E-03	4.3E-03	4.1E-03	5.1E-03
15	2.0E-03	2.5E-02	6.1E-03	4.2E-03	3.5E-03	3.2E-03	3.4E-03
17.5	2.9E-03	1.6E-02	4.6E-03	3.8E-03	3.3E-03	3.1E-03	3.3E-03
20	4.0E-03	1.1E-02	4.5E-03	4.5E-03	4.1E-03	4.1E-03	4.1E-03
22.5	6.1E-03	8.0E-03	6.1E-03	6.2E-03	6.1E-03	6.1E-03	6.0E-03
25	8.7E-03	8.7E-03	8.6E-03	8.7E-03	8.6E-03	8.6E-03	8.6E-03

SNR	Rate1 vs. Rate0	RateST-C2 vs. Rate0	RateST-C3 vs. Rate0	RateST-C4 vs. Rate0	RateST-C4EP vs. Rate0	RateST-QC4 vs. Rate0
0	640%	370%	235%	201%	201%	235%
2.5	467%	283%	192%	169%	169%	192%
5	357%	229%	164%	148%	148%	164%
7.5	270%	185%	143%	132%	132%	143%
10	215%	158%	129%	122%	122%	129%
12.5	176%	138%	119%	114%	114%	119%
15	150%	125%	112%	109%	109%	112%
17.5	131%	115%	108%	106%	106%	108%
20	117%	109%	104%	103%	103%	104%
22.5	105%	103%	101%	101%	101%	101%
25	100%	100%	100%	100%	100%	100%

SNR	Ber1 reference	BerST-C2 vs. Ber1	BerST-C3 vs. Ber1	BerST-C4 vs. Ber1	BerST-C4EP vs. Ber1	BerST-QC4 vs. Ber1
0	100%	60%	46%	38%	41%	50%
2.5	100%	52%	38%	30%	32%	40%
5	100%	44%	30%	22%	24%	31%
7.5	100%	37%	24%	18%	18%	23%
10	100%	30%	20%	14%	14%	18%
12.5	100%	26%	17%	12%	11%	14%
15	100%	25%	17%	14%	13%	14%
17.5	100%	29%	23%	21%	19%	20%
20	100%	42%	42%	38%	38%	38%
22.5	100%	77%	77%	76%	76%	75%
25	100%	99%	100%	99%	99%	99%

Figure C.2: SISO-RA-User1-N4096 experiment setup

MIMO-RA-User1-N512

SNR	rate0	err0	rate1	err1	rateSTC2	errSTC2	rateSTC3	errSTC3	rateSTC4	errSTC4	rateSTC4EP	errSTC4EP	rateSTQC4	errSTQC4	SST
0	84000	0	1020000	96777	552000	20003	318000	5645	258000	3571	258000	1787	316000	4330	234
2.5	152000	1	1020000	45091	584000	6169	368000	1505	314000	994	314000	491	368000	1244	216
5	212000	0	1044000	14550	628000	1051	419000	233	368000	118	368000	86	420000	235	208
7.5	332000	0	1060000	2712	696000	93	512000	17	467000	8	467000	11	512000	23	182
10	536000	0	1108000	274	820000	4	677000	1	641000	0	641000	0	676000	1	142
12.5	816000	0	1200000	38	1008000	0	912000	0	888000	0	888000	0	912000	0	96
15	1260000	0	1344000	4	1300000	0	1281000	0	1275000	0	1275000	0	1280000	0	20
17.5	1728000	0	1732000	0	1728000	0	1728000	0	1728000	0	1728000	0	1728000	0	0
20	2376000	3	2380000	7	2376000	6	2376000	2	2376000	5	2376000	6	2376000	2	0
22.5	3012000	55	3012000	37	3012000	45	3012000	52	3012000	28	3012000	44	3012000	48	0
25	3796000	243	3796000	239	3796000	238	3796000	240	3796000	139	3796000	214	3796000	221	0

SNR	ber0	ber1	berST-C2	berST-C3	berST-C4	berST-C4EP	berST-QC4
0	0	9.5E-02	3.6E-02	1.8E-02	1.4E-02	6.9E-03	1.4E-02
2.5	6.58E-06	4.4E-02	1.1E-02	4.1E-03	3.2E-03	1.6E-03	3.4E-03
5	0	1.4E-02	1.7E-03	5.6E-04	3.2E-04	2.3E-04	5.6E-04
7.5	0	2.6E-03	1.3E-04	3.3E-05	1.7E-05	2.4E-05	4.5E-05
10	0	2.5E-04	4.9E-06	1.5E-06	0	0	1.5E-06
12.5	0	3.2E-05	0	0	0	0	0
15	0	3.0E-06	0	0	0	0	0
17.5	0	0	0	0	0	0	0
20	1.26E-06	2.9E-06	2.5E-06	8.4E-07	2.1E-06	2.5E-06	8.4E-07
22.5	1.83E-05	1.2E-05	1.5E-05	1.7E-05	9.3E-06	1.5E-05	1.6E-05
25	6.40E-05	6.3E-05	6.3E-05	6.3E-05	3.7E-05	5.6E-05	5.8E-05

SNR	Rate1 vs. Rate0	RateST-C2 vs. Rate0	RateST-C3 vs. Rate0	RateST-C4 vs. Rate0	RateST-C4EP vs. Rate0	RateST-QC4 vs. Rate0
0	1214%	657%	379%	307%	307%	376%
2.5	671%	384%	242%	207%	207%	242%
5	492%	296%	198%	174%	174%	198%
7.5	319%	210%	154%	141%	141%	154%
10	207%	153%	126%	120%	120%	126%
12.5	147%	124%	112%	109%	109%	112%
15	107%	103%	102%	101%	101%	102%
17.5	100%	100%	100%	100%	100%	100%
20	100%	100%	100%	100%	100%	100%
22.5	100%	100%	100%	100%	100%	100%
25	100%	100%	100%	100%	100%	100%

SNR	Ber1 reference	BerST-C2 vs. Ber1	BerST-C3 vs. Ber1	BerST-C4 vs. Ber1	BerST-C4EP vs. Ber1	BerST-QC4 vs. Ber1
0	100%	38%	19%	15%	7%	14%
2.5	100%	24%	9%	7%	4%	8%
5	100%	12%	4%	2%	2%	4%
7.5	100%	5%	1%	1%	1%	2%
10	100%	2%	1%	0%	0%	1%
12.5	100%	0%	0%	0%	0%	0%
15	100%	0%	0%	0%	0%	0%
17.5	100%	0%	0%	0%	0%	0%
20	100%	86%	29%	72%	86%	29%
22.5	100%	122%	141%	76%	119%	130%
25	100%	100%	100%	58%	90%	92%

Figure C.3: MIMO-RA-User1-N512 experiment setup

MIMO-RA-User1-N4096

SNR	rate0	err0	rate1	err1	rateSTC2	errSTC2	rateSTC3	errSTC3	rateSTC4	errSTC4	rateSTC4EP	errSTC4EP	rateSTQC4	errSTQC4	SST
0	167000	194	1071000	200223	619000	70002	392750	29636	336500	21426	336500	16082	393000	23436	1808
2.5	238000	288	1108000	160616	673000	50797	455500	21946	401125	15715	401125	11063	455500	16034	1740
5	321000	228	1149500	121959	735000	34255	528000	15055	476250	10133	476250	6934	528000	10036	1656
7.5	458500	471	1233500	95611	846000	23804	652000	11241	603625	7710	603625	5495	652000	7735	1550
10	621000	786	1336500	73749	978500	16537	799875	8570	754875	5788	754875	4698	799500	6228	1430
12.5	832000	1167	1467500	54181	1149500	10838	990625	5956	950875	4134	950875	3764	990500	4580	1270
15	1097000	2291	1641500	40819	1369000	8434	1233125	5429	1199000	4160	1199000	3948	1233000	4406	1088
17.5	1427500	4219	1865000	30003	1646000	7629	1536625	5933	1509250	5317	1509250	5041	1536500	5276	874
20	1819500	7604	2136000	23311	1977500	9358	1898625	8614	1878750	7840	1878750	7800	1898500	7922	632
22.5	2352500	14617	2480500	19817	2416500	14960	2384375	14986	2376500	14601	2376500	14561	2384500	14758	256
25	2954500	26353	2955000	25939	2954500	26367	2954500	26075	2954500	25799	2954500	25891	2954500	25569	0

SNR	ber0	ber1	berST-C2	berST-C3	berST-C4	berST-C4EP	berST-QC4
0	1.2E-03	1.9E-01	1.1E-01	7.5E-02	6.4E-02	4.8E-02	6.0E-02
2.5	1.2E-03	1.4E-01	7.5E-02	4.8E-02	3.9E-02	2.8E-02	3.5E-02
5	7.1E-04	1.1E-01	4.7E-02	2.9E-02	2.1E-02	1.5E-02	1.9E-02
7.5	1.0E-03	7.8E-02	2.8E-02	1.7E-02	1.3E-02	9.1E-03	1.2E-02
10	1.3E-03	5.5E-02	1.7E-02	1.1E-02	7.7E-03	6.2E-03	7.8E-03
12.5	1.4E-03	3.7E-02	9.4E-03	6.0E-03	4.3E-03	4.0E-03	4.6E-03
15	2.1E-03	2.5E-02	6.2E-03	4.4E-03	3.5E-03	3.3E-03	3.6E-03
17.5	3.0E-03	1.6E-02	4.6E-03	3.9E-03	3.5E-03	3.3E-03	3.4E-03
20	4.2E-03	1.1E-02	4.7E-03	4.5E-03	4.2E-03	4.2E-03	4.2E-03
22.5	6.2E-03	8.0E-03	6.2E-03	6.3E-03	6.1E-03	6.1E-03	6.2E-03
25	8.9E-03	8.8E-03	8.9E-03	8.8E-03	8.7E-03	8.8E-03	8.7E-03

SNR	Rate1 vs. Rate0	RateST-C2 vs. Rate0	RateST-C3 vs. Rate0	RateST-C4 vs. Rate0	RateST-C4EP vs. Rate0	RateST-QC4 vs. Rate0
0	641%	371%	235%	201%	201%	235%
2.5	466%	283%	191%	169%	169%	191%
5	358%	229%	164%	148%	148%	164%
7.5	269%	185%	142%	132%	132%	142%
10	215%	158%	129%	122%	122%	129%
12.5	176%	138%	119%	114%	114%	119%
15	150%	125%	112%	109%	109%	112%
17.5	131%	115%	108%	106%	106%	108%
20	117%	109%	104%	103%	103%	104%
22.5	105%	103%	101%	101%	101%	101%
25	100%	100%	100%	100%	100%	100%

SNR	Ber1 reference	BerST-C2 vs. Ber1	BerST-C3 vs. Ber1	BerST-C4 vs. Ber1	BerST-C4EP vs. Ber1	BerST-QC4 vs. Ber1
0	100%	60%	40%	34%	26%	32%
2.5	100%	52%	33%	27%	19%	24%
5	100%	44%	27%	20%	14%	18%
7.5	100%	36%	22%	16%	12%	15%
10	100%	31%	19%	14%	11%	14%
12.5	100%	26%	16%	12%	11%	13%
15	100%	25%	18%	14%	13%	14%
17.5	100%	29%	24%	22%	21%	21%
20	100%	43%	42%	38%	38%	38%
22.5	100%	77%	79%	77%	77%	77%
25	100%	102%	101%	99%	100%	99%

Figure C.4: MIMO-RA-User1-N4096 experiment setup

SISO-LCRA-User1-N512

SNR	rate0	err0	rate1	err1	rateSTC2	errSTC2	rateSTC3	errSTC3	rateSTC4	errSTC4	rateSTC4EP	errSTC4EP	rateSTQC4	errSTQC4	SSTC2
0	92000	0	1020000	96384	556000	20381	323000	7094	266000	4436	266000	4193	324000	9001	232
2.5	148000	0	1020000	45162	584000	6105	364000	1771	310000	1047	310000	800	364000	1999	218
5	232000	0	1052000	14495	640000	1079	436000	288	385000	178	385000	134	436000	330	204
7.5	352000	0	1064000	2536	708000	111	529000	33	484000	11	484000	10	528000	35	178
10	540000	0	1108000	255	824000	9	681000	2	645000	0	645000	0	680000	0	142
12.5	808000	0	1196000	22	1000000	0	904000	0	880000	0	880000	0	904000	0	96
15	1180000	0	1324000	6	1252000	0	1216000	0	1207000	0	1207000	0	1216000	0	36
17.5	1696000	0	1700000	0	1696000	0	1696000	0	1696000	0	1696000	0	1696000	1	0
20	2296000	5	2300000	3	2296000	4	2296000	2	2296000	2	2296000	4	2296000	1	0
22.5	3000000	49	3000000	78	3000000	56	3000000	47	3000000	78	3000000	47	3000000	46	0
25	3752000	255	3752000	242	3752000	251	3752000	228	3752000	268	3752000	202	3752000	236	0

SNR	ber0	ber1	berST-C2	berST-C3	berST-C4	berST-C4EP	berST-QC4
0	0	9.4E-02	3.7E-02	2.2E-02	1.7E-02	1.6E-02	2.8E-02
2.5	0	4.4E-02	1.0E-02	4.9E-03	3.4E-03	2.6E-03	5.5E-03
5	0	1.4E-02	1.7E-03	6.6E-04	4.6E-04	3.5E-04	7.6E-04
7.5	0	2.4E-03	1.6E-04	6.2E-05	2.3E-05	2.1E-05	6.6E-05
10	0	2.3E-04	1.1E-05	2.9E-06	0	0	0
12.5	0	1.8E-05	0	0	0	0	0
15	0	4.5E-06	0	0	0	0	0
17.5	0	0	0	0	0	0	5.9E-07
20	2.18E-06	1.3E-06	1.7E-06	8.7E-07	8.7E-07	1.7E-06	4.4E-07
22.5	1.63E-05	2.6E-05	1.9E-05	1.6E-05	2.6E-05	1.6E-05	1.5E-05
25	6.80E-05	6.4E-05	6.7E-05	6.1E-05	7.1E-05	5.4E-05	6.3E-05

SNR	Rate1 vs. Rate0	RateST-C2 vs. Rate0	RateST-C3 vs. Rate0	RateST-C4 vs. Rate0	RateST-C4EP vs. Rate0	RateST-QC4 vs. Rate0
0	1109%	604%	351%	289%	289%	352%
2.5	689%	395%	246%	209%	209%	246%
5	453%	276%	188%	166%	166%	188%
7.5	302%	201%	150%	138%	138%	150%
10	205%	153%	126%	119%	119%	126%
12.5	148%	124%	112%	109%	109%	112%
15	112%	106%	103%	102%	102%	103%
17.5	100%	100%	100%	100%	100%	100%
20	100%	100%	100%	100%	100%	100%
22.5	100%	100%	100%	100%	100%	100%
25	100%	100%	100%	100%	100%	100%

SNR	Ber1 reference	BerST-C2 vs. Ber1	BerST-C3 vs. Ber1	BerST-C4 vs. Ber1	BerST-C4EP vs. Ber1	BerST-QC4 vs. Ber1
0	100%	39%	23%	18%	17%	29%
2.5	100%	24%	11%	8%	6%	12%
5	100%	12%	5%	3%	3%	5%
7.5	100%	7%	3%	1%	1%	3%
10	100%	5%	1%	0%	0%	0%
12.5	100%	0%	0%	0%	0%	0%
15	100%	0%	0%	0%	0%	0%
17.5	100%	0%	0%	0%	0%	0%
20	100%	134%	67%	67%	134%	33%
22.5	100%	72%	60%	100%	60%	59%
25	100%	104%	94%	111%	83%	98%

Figure C.5: SISO-LCRA-User1-N512 experiment setup

SISO-LCRA-User1-N4096

SNR	rate0	err0	rate1	err1	rateSTC2	errSTC2	rateSTC3	errSTC3	rateSTC4	errSTC4	rateSTC4EP	errSTC4EP	rateSTQC4	errSTQC4	SST
0	163000	193	1069500	198877	616000	69254	389500	33268	332875	23444	332875	25315	389500	36521	1812
2.5	234000	251	1107500	160621	670500	50492	452250	24870	397500	17163	397500	18355	452000	26386	1746
5	329500	309	1153500	123804	741500	34908	535375	17262	484000	11693	484000	12338	535500	17564	1648
7.5	455500	439	1232500	95175	844000	24077	649750	12085	601000	8134	601000	8098	649500	11462	1554
10	618000	844	1334500	73678	976000	16588	796875	8744	752250	5843	752250	5753	797000	7828	1432
12.5	826000	1129	1463500	53494	1144500	10714	985375	5876	945250	4014	945250	3858	985000	4714	1274
15	1089500	2151	1635500	40506	1362500	8220	1226000	5262	1191875	3804	1191875	3628	1226000	4243	1092
17.5	1417500	3927	1860500	29762	1639000	7246	1528125	5891	1500375	4963	1500375	4874	1528000	5005	886
20	1823500	7489	2139500	23551	1981500	9087	1902250	8419	1882750	8058	1882750	7687	1902500	7845	632
22.5	2321500	13279	2464000	18984	2392500	13707	2357125	13740	2348125	13314	2348125	13209	2357000	13208	284
25	2945000	24634	2945500	24692	2945000	25171	2945000	24475	2945000	24572	2945000	24883	2945000	24611	0

SNR	ber0	ber1	berST-C2	berST-C3	berST-C4	berST-C4EP	berST-QC4
0	1.2E-03	1.9E-01	1.1E-01	8.5E-02	7.0E-02	7.6E-02	9.4E-02
2.5	1.1E-03	1.5E-01	7.5E-02	5.5E-02	4.3E-02	4.6E-02	5.8E-02
5	9.4E-04	1.1E-01	4.7E-02	3.2E-02	2.4E-02	2.5E-02	3.3E-02
7.5	9.6E-04	7.7E-02	2.9E-02	1.9E-02	1.4E-02	1.3E-02	1.8E-02
10	1.4E-03	5.5E-02	1.7E-02	1.1E-02	7.8E-03	7.6E-03	9.8E-03
12.5	1.4E-03	3.7E-02	9.4E-03	6.0E-03	4.2E-03	4.1E-03	4.8E-03
15	2.0E-03	2.5E-02	6.0E-03	4.3E-03	3.2E-03	3.0E-03	3.5E-03
17.5	2.8E-03	1.6E-02	4.4E-03	3.9E-03	3.3E-03	3.2E-03	3.3E-03
20	4.1E-03	1.1E-02	4.6E-03	4.4E-03	4.3E-03	4.1E-03	4.1E-03
22.5	5.7E-03	7.7E-03	5.7E-03	5.8E-03	5.7E-03	5.6E-03	5.6E-03
25	8.4E-03	8.4E-03	8.5E-03	8.3E-03	8.3E-03	8.4E-03	8.4E-03

SNR	Rate1 vs. Rate0	RateST-C2 vs. Rate0	RateST-C3 vs. Rate0	RateST-C4 vs. Rate0	RateST-C4EP vs. Rate0	RateST-QC4 vs. Rate0
0	656%	378%	239%	204%	204%	239%
2.5	473%	287%	193%	170%	170%	193%
5	350%	225%	162%	147%	147%	163%
7.5	271%	185%	143%	132%	132%	143%
10	216%	158%	129%	122%	122%	129%
12.5	177%	139%	119%	114%	114%	119%
15	150%	125%	113%	109%	109%	113%
17.5	131%	116%	108%	106%	106%	108%
20	117%	109%	104%	103%	103%	104%
22.5	106%	103%	102%	101%	101%	102%
25	100%	100%	100%	100%	100%	100%

SNR	Ber1 reference	BerST-C2 vs. Ber1	BerST-C3 vs. Ber1	BerST-C4 vs. Ber1	BerST-C4EP vs. Ber1	BerST-QC4 vs. Ber1
0	100%	60%	46%	38%	41%	50%
2.5	100%	52%	38%	30%	32%	40%
5	100%	44%	30%	23%	24%	31%
7.5	100%	37%	24%	18%	17%	23%
10	100%	31%	20%	14%	14%	18%
12.5	100%	26%	16%	12%	11%	13%
15	100%	24%	17%	13%	12%	14%
17.5	100%	28%	24%	21%	20%	20%
20	100%	42%	40%	39%	37%	37%
22.5	100%	74%	76%	74%	73%	73%
25	100%	102%	99%	100%	101%	100%

Figure C.6: SISO-LCRA-User1-N4096 experiment setup

MIMO-LCRA-User1-N512

SNR	rate0	err0	rate1	err1	rateSTC2	errSTC2	rateSTC3	errSTC3	rateSTC4	errSTC4	rateSTC4EP	errSTC4EP	rateSTQC4	errSTQC4	SST
0	92000	0	1020000	97042	556000	20067	323000	5694	266000	3801	266000	2044	324000	4911	232
2.5	148000	0	1020000	45303	584000	6147	364000	1493	310000	946	310000	496	364000	1208	218
5	232000	1	1048000	14717	640000	1136	436000	270	385000	167	385000	113	436000	280	204
7.5	352000	0	1064000	2716	708000	96	529000	26	484000	14	484000	8	528000	26	178
10	540000	0	1108000	266	824000	6	681000	0	645000	1	645000	0	680000	2	142
12.5	812000	0	1196000	31	1004000	0	908000	0	884000	0	884000	0	908000	0	96
15	1184000	0	1324000	6	1252000	0	1217000	0	1208000	0	1208000	0	1216000	0	34
17.5	1696000	0	1700000	0	1696000	0	1696000	0	1696000	0	1696000	0	1696000	2	0
20	2300000	1	2304000	1	2300000	1	2300000	4	2300000	0	2300000	1	2300000	1	0
22.5	2996000	45	2996000	50	2996000	55	2996000	45	2996000	51	2996000	57	2996000	56	0
25	3752000	229	3752000	221	3752000	212	3752000	225	3752000	245	3752000	252	3752000	232	0

SNR	ber0	ber1	berST-C2	berST-C3	berST-C4	berST-C4EP	berST-QC4
0	0	9.5E-02	3.6E-02	1.8E-02	1.4E-02	7.7E-03	1.5E-02
2.5	0	4.4E-02	1.1E-02	4.1E-03	3.1E-03	1.6E-03	3.3E-03
5	4.3E-06	1.4E-02	1.8E-03	6.2E-04	4.3E-04	2.9E-04	6.4E-04
7.5	0	2.6E-03	1.4E-04	4.9E-05	2.9E-05	1.7E-05	4.9E-05
10	0	2.4E-04	7.3E-06	0	1.6E-06	0	2.9E-06
12.5	0	2.6E-05	0	0	0	0	0
15	0	4.5E-06	0	0	0	0	0
17.5	0	0	0	0	0	0	1.2E-06
20	4.3E-07	4.3E-07	4.3E-07	1.7E-06	0.0E+00	4.3E-07	4.3E-07
22.5	1.5E-05	1.7E-05	1.8E-05	1.5E-05	1.7E-05	1.9E-05	1.9E-05
25	6.1E-05	5.9E-05	5.7E-05	6.0E-05	6.5E-05	6.7E-05	6.2E-05

SNR	Rate1 vs. Rate0	RateST-C2 vs. Rate0	RateST-C3 vs. Rate0	RateST-C4 vs. Rate0	RateST-C4EP vs. Rate0	RateST-QC4 vs. Rate0
0	1109%	604%	351%	289%	289%	352%
2.5	689%	395%	246%	209%	209%	246%
5	452%	276%	188%	166%	166%	188%
7.5	302%	201%	150%	138%	138%	150%
10	205%	153%	126%	119%	119%	126%
12.5	147%	124%	112%	109%	109%	112%
15	112%	106%	103%	102%	102%	103%
17.5	100%	100%	100%	100%	100%	100%
20	100%	100%	100%	100%	100%	100%
22.5	100%	100%	100%	100%	100%	100%
25	100%	100%	100%	100%	100%	100%

SNR	Ber1 reference	BerST-C2 vs. Ber1	BerST-C3 vs. Ber1	BerST-C4 vs. Ber1	BerST-C4EP vs. Ber1	BerST-QC4 vs. Ber1
0	100%	38%	19%	15%	8%	16%
2.5	100%	24%	9%	7%	4%	7%
5	100%	13%	4%	3%	2%	5%
7.5	100%	5%	2%	1%	1%	2%
10	100%	3%	0%	1%	0%	1%
12.5	100%	0%	0%	0%	0%	0%
15	100%	0%	0%	0%	0%	0%
17.5	100%	0%	0%	0%	0%	0%
20	100%	100%	401%	0%	100%	100%
22.5	100%	110%	90%	102%	114%	112%
25	100%	96%	102%	111%	114%	105%

Figure C.7: MIMO-LCRA-User1-N512 experiment setup

MIMO-LCRA-User1-N4096

SNR	rate0	err0	rate1	err1	rateSTC2	errSTC2	rateSTC3	errSTC3	rateSTC4	errSTC4	rateSTC4EP	errSTC4EP	rateSTQC4	errSTQC4	SST
0	163000	211	1068500	199540	615500	69493	389125	29832	332500	21164	332500	15770	389000	23032	1810
2.5	234000	249	1107000	160714	670500	51431	452250	22079	397500	15279	397500	10884	452000	15805	1746
5	330000	285	1154000	123966	742000	34831	535875	15475	484500	10347	484500	7393	536000	10410	1648
7.5	456000	443	1232000	95161	844000	24024	649875	11218	601500	7439	601500	5562	650000	7541	1552
10	618500	769	1335500	74477	977000	16664	797750	8428	752750	5648	752750	4762	797500	6215	1434
12.5	826000	1188	1463500	53543	1144500	10631	985375	5787	945250	4001	945250	3555	985000	4653	1274
15	1089500	2071	1636500	39785	1363000	7684	1226000	5036	1191875	3778	1191875	3558	1226000	4042	1094
17.5	1417500	3975	1860500	29889	1639000	7430	1528125	5697	1500375	5031	1500375	4905	1528000	5156	886
20	1824000	7638	2139500	23205	1981500	9649	1902750	8491	1882875	8200	1882875	8081	1902500	8315	630
22.5	2323000	13584	2465000	19259	2394000	14170	2358250	13727	2349625	13769	2349625	13734	2358500	14109	284
25	2945500	25048	2946000	24971	2945500	25235	2945500	24779	2945500	25597	2945500	25160	2945500	24978	0

SNR	ber0	ber1	berST-C2	berST-C3	berST-C4	berST-C4EP	berST-QC4
0	1.3E-03	1.9E-01	1.1E-01	7.7E-02	6.4E-02	4.7E-02	5.9E-02
2.5	1.1E-03	1.5E-01	7.7E-02	4.9E-02	3.8E-02	2.7E-02	3.5E-02
5	8.6E-04	1.1E-01	4.7E-02	2.9E-02	2.1E-02	1.5E-02	1.9E-02
7.5	9.7E-04	7.7E-02	2.8E-02	1.7E-02	1.2E-02	9.2E-03	1.2E-02
10	1.2E-03	5.6E-02	1.7E-02	1.1E-02	7.5E-03	6.3E-03	7.8E-03
12.5	1.4E-03	3.7E-02	9.3E-03	5.9E-03	4.2E-03	3.8E-03	4.7E-03
15	1.9E-03	2.4E-02	5.6E-03	4.1E-03	3.2E-03	3.0E-03	3.3E-03
17.5	2.8E-03	1.6E-02	4.5E-03	3.7E-03	3.4E-03	3.3E-03	3.4E-03
20	4.2E-03	1.1E-02	4.9E-03	4.5E-03	4.4E-03	4.3E-03	4.4E-03
22.5	5.8E-03	7.8E-03	5.9E-03	5.8E-03	5.9E-03	5.8E-03	6.0E-03
25	8.5E-03	8.5E-03	8.6E-03	8.4E-03	8.7E-03	8.5E-03	8.5E-03

SNR	Rate1 vs. Rate0	RateST-C2 vs. Rate0	RateST-C3 vs. Rate0	RateST-C4 vs. Rate0	RateST-C4EP vs. Rate0	RateST-QC4 vs. Rate0
0	656%	378%	239%	204%	204%	239%
2.5	473%	287%	193%	170%	170%	193%
5	350%	225%	162%	147%	147%	162%
7.5	270%	185%	143%	132%	132%	143%
10	216%	158%	129%	122%	122%	129%
12.5	177%	139%	119%	114%	114%	119%
15	150%	125%	113%	109%	109%	113%
17.5	131%	116%	108%	106%	106%	108%
20	117%	109%	104%	103%	103%	104%
22.5	106%	103%	102%	101%	101%	102%
25	100%	100%	100%	100%	100%	100%

SNR	Ber1 reference	BerST-C2 vs. Ber1	BerST-C3 vs. Ber1	BerST-C4 vs. Ber1	BerST-C4EP vs. Ber1	BerST-QC4 vs. Ber1
0	100%	60%	41%	34%	25%	32%
2.5	100%	53%	34%	26%	19%	24%
5	100%	44%	27%	20%	14%	18%
7.5	100%	37%	22%	16%	12%	15%
10	100%	31%	19%	13%	11%	14%
12.5	100%	25%	16%	12%	10%	13%
15	100%	23%	17%	13%	12%	14%
17.5	100%	28%	23%	21%	20%	21%
20	100%	45%	41%	40%	40%	40%
22.5	100%	76%	75%	75%	75%	77%
25	100%	101%	99%	103%	101%	100%

Figure C.8: MIMO-LCRA-User1-N4096 experiment setup

Bibliography

[1] Alamouti, S.M. A simple transmit diversity technique for wireless communications. *Selected Areas in Communications, IEEE Journal on*, 16(8):1451–1458, Oct. 1998.

[2] Bin Lee; Cioffi, J.M.; Jagannathan, S.; Kibeom Seong; Youngjae Kim; Mohseni, M.; Brady, M.H. Binder MIMO channels. *Communications, IEEE Transactions on*, 55(8):1617–1628, Aug. 2007.

[3] Bin Lee; Cioffi, J.M.; Jagannathan, S.; Mohseni, M. Gigabit DSL. *Communications, IEEE Transactions on*, 55(9):1689–1692, Sep. 2007.

[4] Bingham, J.A.C. *ADSL, VDSL and Multicarrier Modulation.* A Wiley-Interscience Publication, John Wiley & Sons, Inc., 605 Third Avenue, New York, NY 10158-0012, 2000.

[5] Biyani, P.; Mahadevan, A.; Duvaut, P.; Singh, S. Cooperative MIMO for alien noise cancellation in upstream VDSL. In *Acoustics, Speech and Signal Processing, 2009. ICASSP 2009. IEEE International Conference on*, pages 2645–2648, Apr. 2009.

[6] Cendrillon, R.; Moonen, M.; Suciu, R.; Ginis, G. Simplified power allocation and TX/RX structure for MIMO-DSL. In *Global Telecommunications Conference, 2003. GLOBECOM '03. IEEE*, volume 4, pages 1842–1846, Dec. 2003.

[7] Cendrillon, R.; Moonen, M.; Verliden, J.; Bostoen, T.; Yu Wei. Optimal multi-user spectrum management for digital subscriber lines. *IEEE Transactions on Communications*, 1:1–5, 2004.

[8] Chow, P.S.; Cioffi, J.M.; Bingham, J.A.C. A practical discrete multitone transceiver loading algorithm for data transmission over spectrally shaped channels. *Communications, IEEE Transactions on*, 43(234):773–775, Feb/Mar/Apr 1995.

[9] Cioffi, J.M. Advanced Digital Communication classes. `http://www.stanford.edu/class/ee379c/`, 2007–2008.

[10] Cioffi, J.M.; Al-Dhahir, N.M.W. Efficiently computed reduced-parameter input-aided MMSE equalizers for ML detection: A unified approach. *IEEE Trans. on Information Theory*, 42(3):903–915, May 1996.

[11] Cioffi, J.M.; Jagannathan, S.; Mohseni, M.; Ginis, G. CuPON: the copper alternative to PON 100 Gb/s DSL networks [accepted from open call]. *Communications Magazine, IEEE*, 45(6):132–139, Jun. 2007.

[12] Crussiere, M.; Baudais, J.-Y.; Helard, J.-F. Improved throughput over wirelines with adaptive MC-DS-CDMA. In *Spread Spectrum Techniques and Applications, 2006 IEEE Ninth International Symposium on*, pages 143–147, Aug. 2006.

[13] Duvaut, P.; Mahadevan, A.; Sorbara, M.; Langberg, E.; Biyani, P. Adaptive off-diagonal MIMO pre-coder (ODMP) for downstream DSL self FEXT cancellation. In *Global Telecommunications Conference, 2007. GLOBECOM '07. IEEE*, pages 2910–2915, Nov. 2007.

[14] Eriksson, P.-E.; Cioffi, J.M.; Ginis, G. The path to 100 Mbps DSL services: VDSL2 vectoring performance and deployment aspects. In *IEEE Globecom 2009, Access forum, Session 203*, Dec. 2009.

[15] Foschini, G.J. Layered space-time architecture for wireless communication in a fading environment when using multi-element antennas. *Bell Labs Technical Journal*, 1(2):41–59, 1996.

[16] Foschini, G.J. Layered space-time architecture for wireless communication in a fading environment when using multi-element antennas. *Bell Labs Technical Journal*, 1(2):41–59, 1996.

[17] Ganesan, G. and Stoica, P. Space-time block codes: a maximum SNR approach. *Information Theory, IEEE Transactions on*, 47(4):1650–1656, May 2001.

[18] Gesbert, D.; Shafi,M.; Shiu, D. From theory to practice: An overview of MIMO space-time coded wireless systems. *IEEE on Selected Areas in Communications*, 21(3):281–302, Apr. 2003.

[19] Giannakis, Georgios B.; Liu, Zhiqiang; Ma, Xiaoli; Zhou, Shengli. *Space Time Coding for Broadband Wireless Communications.* A Wiley-Interscience Publication, John Wiley & Sons, Inc., 111 River Street, Hoboken, New Jersey 07030, 2003.

[20] Ginis, G.; Cioffi, J.M. Vectored transmission for digital subscriber line systems. *Selected Areas in Communications, IEEE Journal on*, 20(5):1085–1104, Jun. 2002.

[21] Ginis, G.; Goldburg, M.; Cioffi, J. M. The effects of vectored DSL on network operations. *Journal of Telecommunications Management*, 3(2):107–117, Jul. 2010.

[22] Ginis, G.; Mohseni, M.; Cioffi, J.M. Vectored DSL to the rescue. *OSP Magazine*, Apr. 2010.

[23] Ginis, G.; Peng, C.-N. Alien crosstalk cancellation for multipair digital subscriber line systems. *EURASIP Journal on Applied Signal Processing*, page 12, 2006.

[24] Haykin, S.; Moher, M. *Modern Wireless Communications.* Prentice-Hall, Inc., Upper Saddle River, NJ, USA, 2004.

[25] Hsuan-Jung Su; Geraniotis, E.; Gerakoulis, D.P. Orthogonal code division multiplexed DSL for interference suppression in cable networks. In *Communications, 2000. ICC 2000. 2000 IEEE International Conference on*, volume 2, pages 1069–1074, 2000.

[26] Ibnkahla, M. *Signal Processing for Mobile Communications Handbook*. CRC Press LLC, 2000 N.W. Corporate Blvd., Boca Raton, Florida 33431, 2004.

[27] International Telecommunication Union. ITU-T Recommendation G.992.1: Asymmetric Digital Subscriber Line Transceivers (ADSL). , Jun. 1999.

[28] International Telecommunication Union. ITU-T Recommendation G.992.3: Asymmetric Digital Subscriber Line Transceivers 2 (ADSL2). , Jul 2002.

[29] International Telecommunication Union. ITU-T Recommendation G.993.1: Very high speed digital subscriber line transceivers. , Jun. 2004.

[30] International Telecommunication Union. ITU-T Recommendation G.993.2: Very high speed digital subscriber line transceivers 2 (VDSL2). , Feb. 2006.

[31] International Telecommunication Union. ITU-T Recommendation G.992.5: Asymmetric Digital Subscriber Line (ADSL) transceivers - Extended bandwidth ADSL2 (ADSL2plus). , Jan. 2009.

[32] International Telecommunication Union. ITU-T Recommendation G.993.5: Self-FEXT cancellation (Vectoring) for use with VDSL2 transceivers. , Apr. 2010.

[33] Jafarkhani, H. A quasi-orthogonal space-time block code. *Communications, IEEE Transactions on*, 49(1):1–4, Jan. 2001.

[34] Jagannathan, S.; Pourahmad, V.; Seong, K.; Cioffi, J.; Ouzzif, M.; Tarafi, R. Common-mode data transmission using the binder sheath in digital subscriber lines. *Communications, IEEE Transactions on*, 57(3):831–840, Mar. 2009.

[35] Mohseni, M.; Ginis, G.; Cioffi, J.M. Dynamic spectrum management for mixtures of vectored and non-vectored DSL systems. In *Information Sciences and Systems (CISS), 2010 44th Annual Conference on*, pages 1–6, Mar. 2010.

[36] Ödling, P.; Magesacher, T.; Höst, S.; Börjesson, P.O.; Berg, M.; Areizaga, E. The fourth generation broadband concept. *IEEE Communications Magazine*, 47(1):62–69, Jan. 2009.

[37] Perez-Cruz, F.; Rodrigues, M.R.D.; Verdu, S. Optimal precoding for digital subscriber lines. In *Communications, 2008. ICC '08. IEEE International Conference on*, pages 1200–1204, May 2008.

[38] Raleigh, G.G.; Cioffi, J.M. Spatio-temporal coding for wireless communication. *Communications, IEEE Transactions on*, 46(3):357–366, Mar. 1998.

[39] Sandstrom, L.; Schneider, K.; Joiner, L.; Wilson, A. Spatial correlation of alien crosstalk in MIMO DSL systems. *Communications, IEEE Transactions on*, 57(8):2269–2271, Aug. 2009.

[40] Starr, T.; Sorbara, M.; Cioffi, J. M.; Silverman, P. *DSL Advances*. Prentice Hall PTR, Upper Saddle River, NJ 07458, Dec. 2002.

[41] Tarokh, V.; Jafarkhani, H.; Calderbank, A.R. Space-time block codes from orthogonal designs. *Information Theory, IEEE Transactions on*, 45(5):1456–1467, Jul. 1999.

[42] Tarokh, V.; Jafarkhani, H.; Calderbank, A.R. Space-time block coding for wireless communications: performance results. *Selected Areas in Communications, IEEE Journal on*, 17(3):451–460, Mar. 1999.

[43] Tsiaflakis, P.; Diehl, M.; Moonen, M. Distributed spectrum management algorithms for multiuser DSL networks. *Signal Processing, IEEE Transactions on*, 56(10):4825 –4843, Oct. 2008.

[44] Van Acker, K. Equalization and Echo Cancellation for DMT Modems. SISTA-ESAT K.U. Leuven, Belgium, Jan. 2001.

[45] van Wyk, J.; Linde, L. Design of a CC-MC-CDMA system for gigabit DSL (GDSL). In *Information Technology: New Generations, 2009. ITNG '09. Sixth International Conference on*, pages 883–888, Apr. 2009.

[46] van Wyk, J.H.; Linde, L.P. Combatting multi-user interference in ADSL systems using time-spreading. In *Electrical and Computer Engineering, 2003. IEEE CCECE 2003. Canadian Conference on*, volume 1, pages 155–158, May. 2003.

[47] Ysebaert, G. Equalization and Echo Cancellation in DMT-based Systems. SISTA-ESAT K.U. Leuven, Belgium, Apr. 2004.

List of Figures

List of Tables